MOL #8417R

# β-arrestin Dependent Spontaneous $\alpha_{1a}$-Adrenoceptor Endocytosis causes Intracellular Transportation of α-blockers via Recycling Compartments

John D. Pediani, Janet F. Colston, Darren Caldwell, Graeme Milligan, Craig J. Daly and John C. McGrath

Autonomic Physiology Unit, Division of Neuroscience and Biomedical Systems, Institute of Biomedical and Life Sciences, University of Glasgow, Glasgow G12 8QQ, Scotland, U.K. (J.D.P., J.F.C., D.C., C.J.D., J.C.M); Molecular Pharmacology Group, Division of Biochemistry and Molecular Biology, Institute of Biomedical and Life Sciences, University of Glasgow, Glasgow G12 8QQ, Scotland, U.K. (G. M.)

Molecular Pharmacology Fast Forward. Published on December 30, 2004 as DOI: 10.1124/mol.104.008417
This article has not been copyedited and formatted. The final version may differ from this version.

MOL #8417R

Running title: Spontaneous recycling of the $\alpha_{1a}$-adrenoceptor

Corresponding author: John Pediani

Autonomic Physiology Unit, Institute of Biomedical and Life Sciences, University of Glasgow, Glasgow G12 8QQ, Scotland, U.K.

Phone: 44 (0) 141 330 6606; FAX: 44 (0) 141 330 2923; john.pediani@bio.gla.ac.uk

Manuscript Information:

Text pages:38

Tables: 2

Figures:9

References: 40

Abstract words: 247.

Introduction words: 503.

Discussion words: 1913

**Abbreviations:** $\alpha_1$-AR, alpha 1-adrenoceptor; Con A, concanavalin A; DMEM, Dulbecco's modification of Eagle's medium; EGFP, enhanced green fluorescent protein; GPCR, G-protein coupled receptor; HEK293, human embryonic kidney cells; HEPES, 4-(2-hydroxyethyl)-1-piperazine sulphonic acid; MEFs, mouse embryo fibroblasts; R-1F, Rat-1 fibroblast; PBS, phosphate-buffered saline; QAPB, BODIPY-FL prazosin; RQAPB, BODIPY-R 558/568 prazosin; Tfn, Transferrin.

Molecular Pharmacology Fast Forward. Published on December 30, 2004 as DOI: 10.1124/mol.104.008417
This article has not been copyedited and formatted. The final version may differ from this version.



**ABSTRACT**

The antagonist ligand BODIPY-FL-prazosin (QAPB) fluoresces when bound to bovine $\alpha_{1a}$-adrenoceptors (ARs). Data indicates that the receptor-ligand complex is spontaneously internalized by β-arrestin-dependent endocytosis. Internalization of the ligand did not occur in β-arrestin-deficient cells, was blocked or reversed by another $\alpha_1$ ligand, phentolamine, indicating it to reflect binding to the orthosteric recognition site, and was prevented by blocking clathrin-mediated endocytosis. The ligand showed rapid, diffuse, low-intensity, surface binding, superseded by punctate intracellular binding that developed to equilibrium in 50-60 min, and was reversible on ligand removal, indicating a dynamic equilibrium. In cells expressing a human $\alpha_{1a}$-AR-EGFP2 fusion protein, BODIPY-R-558/568-prazosin (RQAPB) co-localized with the fusion, indicating that the ligand gained access to all compartments containing the receptor and, conversely, that the receptor has affinity for the ligand at all of these sites. The distribution of QAPB binding sites was similar for receptors with or without EGFP2, validating the fusion protein as an indicator of receptor location. The ligand partially co-localized with β-arrestin in recycling and late endosomes indicating receptor transit without destruction. Organelles containing receptors showed considerable movement consistent with a transportation function. This was absent in β-arrestin-deficient cells indicating that both constitutive receptor internalization and subsequent intracellular transportation are β-arrestin-dependent. Calculations of relative receptor number indicate that at steady-state less than 30% of receptors reside on the cell surface and that recycling is rapid. We conclude that $\alpha_{1a}$-ARs recycle rapidly by an agonist-independent, constitutive, β-arrestin-dependent process and that this can transport "α-blockers" into cells carrying these receptors.

Molecular Pharmacology Fast Forward. Published on December 30, 2004 as DOI: 10.1124/mol.104.008417
This article has not been copyedited and formatted. The final version may differ from this version.



**INTRODUCTION**

We have observed in live smooth muscle cells expressing $\alpha_1$-ARs that a fluorescent antagonist ligand, the prazosin analogue QAPB, labels intracellular receptors. This process takes longer than expected of simple diffusion, suggesting an uptake process (Mackenzie *et al*., 2000). It is known that fluorescent agonists can be internalized while bound to the receptors that they activate (Kallal and Benovic, 2000; Kallal and Benovic, 2002; Daly and McGrath, 2003). It is also possible that antagonists of receptor-mediated second messenger regulation can also initiate internalization, as shown previously for the cholecystokinin receptor (Roettger *et al*., 1997). However, an antagonist ligand might be internalized simply by binding to a receptor that is spontaneously recycling. Morris *et al*., (2004) recently showed that when expressed in rat-1 fibroblasts (R-1Fs) the human $\alpha_{1a}$-AR can internalize spontaneously by using antibodies to an extracellular epitope to follow the receptors, excluding the possibility of internalization through occupation of the receptive site.

We now show that antagonists such as QAPB can be internalized bound to spontaneously recycling $\alpha_{1a}$-ARs and analyse the mechanisms involved. QAPB is a prazosin analogue in which the furan ring has been substituted by a BODIPY fluorescent moiety. It retains prazosin's high affinity, functional antagonism and relative selectivity for $\alpha_1$-ARs, and, like prazosin, does not distinguish within the family of three $\alpha_1$-AR subtypes. Importantly for its present use, it fluoresces when bound to the receptor in live cells yet remains essentially non-fluorescent in the aqueous phase. This allows quantitative visual assessment of its binding to receptors at equilibrium (Daly *et al*., 1998). It has been employed to measure binding affinity at recombinant and native $\alpha_1$-ARs in different regions of cultured cells and of freshly dissociated cells from human and other mammalian tissue (McGrath *et al*., 1996; Daly *et al*., 1998; McGrath *et al*., 1999; Mackenzie *et al*., 2000). We have quantified the pharmacology of agonist and antagonist interaction at recombinant $\alpha_1$-AR in R-1Fs (Pediani *et al*., 2000), demonstrating that the receptors are functional and have the predicted pharmacology. This cell line provides the main basis for the present study. We accomplished real-time visualization of antagonist-receptor binding interactions in a concentration range near to the ligand's dissociation constant. Binding was found at intracellular sites as well as on the cell surface. We further established the utility of the fluorescent ligand by demonstrating co-localization of the QAPB-receptor complex and receptors tagged with the auto-fluorescent green fluorescent protein variant EGFP2. These independent measures of receptor location allowed us to cross-validate the fluorescent ligand as reflecting the

Molecular Pharmacology Fast Forward. Published on December 30, 2004 as DOI: 10.1124/mol.104.008417
This article has not been copyedited and formatted. The final version may differ from this version.



localization of receptor binding sites and the EGFP2 as indicating the presence of receptors that could bind antagonists. We investigated the mechanism by which the ligand entered the cell by blocking internalization processes and used vital organelle markers to identify the compartments in which the $\alpha_{1a}$-AR-ligand fluorescent complex resides. Analysis of the contribution of β-arrestin indicated that $\alpha_{1a}$-AR spontaneously recycle in a β-arrestin-dependent but agonist-independent manner. The rate of uptake and cellular distribution of the ligand-receptor complex was used to estimate the turnover of the spontaneous recycling process.

Molecular Pharmacology Fast Forward. Published on December 30, 2004 as DOI: 10.1124/mol.104.008417
This article has not been copyedited and formatted. The final version may differ from this version.



## MATERIAL AND METHODS

**Materials.** Cell culture plastics were supplied by Falcon or Packard. Dulbecco's modification of Eagle's medium (DMEM) with sodium pyruvate, new-born calf serum, L-glutamine, penicillin, streptomycin, active geneticin (50mg/ml), trypsin/ethylenediamine tetra-acetic acid, pCDNA3 and Dulbecco's phosphate-buffered saline (PBS) were purchased from Invitrogen (Paisley, Scotland). The pEGFP2 N2 vector was purchased from Packard Biosciences (Berkshire, UK). HEPES, sucrose, phenylephrine, phentolamine, concanavalin A, (Con A) and filipin were purchased from Sigma (Dorset, UK). Prazosin HCl was supplied by Research Biochemicals Incorporated (RBI) and [$^3$H]-prazosin (0.2 nM; specific activity, 76 Ci/mmol) was from Amersham Corp. (Arlington Heights, IL). Hoechst 33342, BODIPY-FL labeled prazosin (QAPB), BODIPY-R 558/568 labeled prazosin (RQAPB), lysotracker Red DND-99 and Transferrin-Alexa Fluor$^{546}$ were purchased from Molecular Probes (Molecular Probes, Eugene, OR). All optical fluorescence filters were purchased from Chroma Technology Corp. (Rockingham, VT).

Stock solutions for each chemical were prepared in distilled water or dimethyl sulphoxide and subsequently aliquoted and stored at -20°C. These stock solutions were diluted to working concentrations in physiological salt solution on each experimental day.

**Construction of plasmids.** Production and subcloning of $\alpha_{1a}$-AR-EGFP2 involved PCR amplification of the human $\alpha_{1a}$-AR sequence using the amino-terminal primer 5'- AAA AGG TAC CAT GGT GTT TCT CTC GGG AAA TGC TTC -3' to introduce a *Kpn*1 restriction sequence upstream of the coding sequence. Using the carboxyl-terminal primer 5'-AAA AGG ATC CGA CTT CCT CCC CGT TCT CAC TGA GGG -3' the receptor stop codon was removed and a *Bam*H1 restriction enzyme site was introduced downstream of the receptor coding sequence. The resulting PCR fragments were then ligated either into the multiple cloning site of the pEGFP2 N2 vector (Packard Biosciences) or the expression vector pcDNA3 (Invitrogen) to form the EGFP2 tagged and non EGFP2 labelled version of the human $\alpha_{1a}$-AR respectively. Each construct was fully sequenced before its expression and analysis. β-arrestin-2-EGFP was obtained from Dr. C. Krasel (Department of Pharmacology, University of Würzburg, Germany).

**Cell culture and transfection.** R-1Fs stably expressing the bovine $\alpha_{1a}$-AR were grown in DMEM supplemented with 5% (vol./vol.) new-born calf serum, penicillin (100 i.u. ml), streptomycin (100 μg/ml) and L-glutamine (1 mM) in a 95% air and 5% $CO_2$ atmosphere at 37°C. Selection was maintained by adding geneticin (400 μg/ml) to the growth media.

HEK293T cells were maintained in DMEM supplemented with 0.292 g/L L-glutamine and 10% (v/v) newborn calf serum and incubated at 37°C with 5% $CO_2$. HEK293T cells were grown on glass coverslips to ~70% confluency before transient transfection with the appropriate human $\alpha_{1a}$-AR plasmid using LipofectAMINE reagent (Invitrogen). After 4 h, cells were washed twice with Opti-MEM I and cultured in DMEM for 24 h. A total of 3 μg of pEGFP2 N2 vector or pCDNA3 containing the human $\alpha_{1a}$-AR cDNA was used to transfect each coverslip. Mouse embryo fibroblasts (MEFs) derived from both wild type and β-arrestin 1 plus β-arrestin 2 knock-out animals have been described previously (Kohout *et al*., 2001) and were obtained from Dr. R.J. Lefkowitz, Duke University, Durham, NC. These were maintained in DMEM supplemented with 0.292g/l L-glutamine and 10 % (v/v) foetal-calf serum at 37 °C in a 5 % $CO_2$ environment. Cells were grown to 60-80 % confluency prior to transient transfection on sterile glass coverslips. Transfection, (3 μg of cDNA), was carried out using the AMAXA nucleofector system (Cologne, Germany) according to the manufacturer's instructions using program T20.

**Radioligand binding.** Competitive $\alpha_1$-AR binding assays were performed as previously described (MacKenzie *et al*., 2000). Briefly, R-1F homogenates (0.05 mg/ml) stably expressing the bovine $\alpha_{1a}$-AR were incubated in triplicate with the non-selective $\alpha_1$-AR antagonist [$^3$H]-prazosin (0.2 nM) in the presence or absence of a range of increasing concentrations of competing ligands in a total volume of 0.5 ml Tris HCl assay buffer. Non-specific binding was determined as radioligand binding in the presence of 10 μM phentolamine. All equilibrations were carried out for 30 min at 25°C and bound ligand was separated from free by rapid cold vacuum filtration over Whatman GF/C filters (Whatman International Ltd, Maidstone, U.K.) using a Brandell cell harvester. Concentrations of displacing agent eliciting 50% displacement of [$^3$H]-prazosin ($IC_{50}$) were interpolated with the use of non-linear iterative curve fitting methodologies performed by PRISM 4.02, (GraphPAD Software, San Diego, CA) and converted into $pK_i$ with the equation of Cheng and Prussoff (1973).

Molecular Pharmacology Fast Forward. Published on December 30, 2004 as DOI: 10.1124/mol.104.008417
This article has not been copyedited and formatted. The final version may differ from this version.



**Fluorescence experiments undertaken in R-1Fs**

**Epifluorescence imaging of QAPB binding to spontaneously recycling bovine $\alpha_{1a}$-ARs.** R-1Fs stably expressing the bovine $\alpha_{1a}$-AR were grown on sterile coverslips 24 h before experimentation. Coverslips were mounted into a flow chamber, placed on to the microscope stage and superfused, (5 ml/min) with HEPES buffered saline solution at room temperature. Cells were illuminated using an ultra high point intensity 75 W xenon arc lamp (Optosource, Cairn Research, Faversham, Kent, UK). A Nikon Diaphot inverted microscope equipped with a 40 x oil immersion Fluor objective lens (NA=1.3) and a monochromator (Optoscan, Cairn Research, Faversham, Kent, UK) set at an excitation wavelength of 490 nm (band pass=7 nm) was used to determine the background autofluorescence. After acquiring the background autofluorescence, the cells were superfused with fresh saline supplemented with the fluorescent antagonist ligand QAPB (5 nM) until equilibrium binding of QAPB occurred. QAPB fluorescence emission was detected by a cooled digital CCD camera, (Cool Snap-HQ, Roper Scientific/Photometrics, Tucson, AZ). MetaFluor imaging software (version 4.6.9; Universal Imaging Corp., Downing, PA) was used for control of the monochromator, CCD camera, for processing of all the cell image data and movie animations.

Sequential QAPB images (2 x 2 binning) were collected at 5 sec intervals to determine the total QAPB fluorescence intensity associated with each cell and exposure to excitation light was 60 msec/image. QAPB binding to $\alpha_{1a}$-ARs was time dependently reversed by washing with QAPB ligand-free saline solution, with or without 100μM phentolamine, (the latter incorporated to prevent rebinding of dissociating ligand and, therefore, to approximate infinite dilution conditions).

**Quantification of the fraction of QAPB ligand receptor complexes that are intracellular versus surface at steady state.** Receptor expression at the cell surface, (i.e. cell membrane, clathrin-coated pits) was defined as the rapid, initial, diffuse QAPB fluorescence that occurs after ligand addition, but before the fluorescent ligand-receptor-containing endocytic vesicles can be visually resolved. Subtraction of the cell surface fluorescence from the total fluorescence allowed us to determine the intracellular fluorescence and the maximal intracellular fluorescence was normalized to the maximal total QAPB fluorescence measured at steady state.

The rate of development of QAPB associated or dissociated fluorescence was determined by fitting one phase exponential association or dissociation equations, (via non-linear regression), to each data point,

(GraphPAD Software, San Diego, CA). The reciprocal of the rate constant was used to determine t½ values.

**Reversal of QAPB fluorescence binding to $\alpha_{1a}$-ARs by the competitive $\alpha_1$-antagonist ligand phentolamine** Spontaneously recycling $\alpha_{1a}$-ARs were pre-equilibrated with QAPB (5 nM) for 75 min at room temperature before an image was acquired to determine the total QAPB fluorescence intensity associated with each R-1F. Sequential QAPB images (2 x 2 binning, 60 msec/image) were collected at 15 sec intervals for a further 15 min to determine that equilibrium binding of QAPB had taken place prior to superfusion of the cells with saline containing QAPB (5 nM) plus phentolamine (10 μM). R-1Fs were equilibrated with this solution until the ligands QAPB and phentolamine had reached their new steady-state receptor occupancies. The remaining QAPB associated fluorescence was then time-dependently removed by exposing the cells to saline containing the same concentration of QAPB (5 nM) plus a higher concentration of phentolamine (100 μM).

Using the editing capability of MetaFluor, QAPB intensity values derived from groups of R-1Fs were obtained by manually delimiting the profile of the cells and averaging the signals within the delimited region of interest for each time lapse image captured. These averaged QAPB intensity values were exported into PRISM 4.02, (GraphPAD Software, San Diego, CA) and plotted over time.

**Histogram intensity plots.** Binned pixel intensities, (8 bit image of 256 intensities divided into 9 intensity bins), of fluorescence histogram**s** representative of the localization of QAPB labelled $\alpha_{1a}$-ARs, (over time), were computed using the histogram plot profile tool of MetaMorph 6.2.6 software. Background subtracted image acquired at 0 sec was determined as cell autofluorescence and the pixel intensity of membrane QAPB fluorescence was calculated as the diffuse fluorescence that was observed after 2 min exposure to the ligand. To remove contributions of the plasma membrane signal into the intracellular QAPB signal, the diffuse fluorescence observed at 2 min was subtracted from all subsequently acquired images.

Binned integral counts acquired at various time intervals after addition or removal of the QAPB ligand were measured and expressed as intensity integral counts. QAPB binding to $\alpha_{1a}$-ARs was detected as a shift to the right of the autofluorescence plot (at 0 sec) and the quantified histogram data was used for comparison of intensity in various structures within the image data. Loss of QAPB from cycling $\alpha_{1a}$-

Molecular Pharmacology Fast Forward. Published on December 30, 2004 as DOI: 10.1124/mol.104.008417
This article has not been copyedited and formatted. The final version may differ from this version.



ARs was detected as a progressive shift to the left of the fluorescence intensity measured at equilibrium.

**Image analysis colocalization**

For the analysis of RQAPB-labelled bovine $\alpha_{1a}$-ARs with β-arrestin-2-EGFP2, a region of no fluorescence adjacent to the cell was used to determine the average background level of fluorescence in the EGFP2 and RQAPB channels. The background amount was then subtracted from each pixel in each channel. Using the editing capability of MetaFluor, QAPB intensity values derived from groups of R-1Fs were obtained by manually delimiting the profile of the cells. Using the editing function a region of interest was manually drawn in the EGFP2 channel image, then selected and transferred to the matched image acquired in the RQAPB channel. Correlation coefficients were evaluated by comparing the amounts of fluorescence measured in each matched pixel of the two different channels using the Metamorph "correlation plot" application.

**Blockade and reversal of QAPB fluorescence binding to recycling $\alpha_{1a}$-ARs by concanavalin A and hyperosmotic sucrose, but not filipin.** To study the role of clathrin-coated vesicles and caveolae in $\alpha_{1a}$-AR endocytosis, the effects of hyperosmotic sucrose, concanavalin A (Con A) and filipin on QAPB binding to recycling $\alpha_{1a}$-ARs was assessed as follows: R-1Fs were superfused with saline and a background autofluorescence image was acquired. R-1Fs were then pre-equilibrated with QAPB (5 nM) for 90 min at room temperature, which was sufficient time for QAPB binding to $\alpha_{1a}$-ARs to reach equilibrium. An image was then acquired to determine the total QAPB fluorescence intensity. QAPB fluorescence was then completely removed by superfusing the cells with ligand-free saline for 90 min and a background autofluorescence image was acquired. The R-1Fs were re-exposed to control saline or saline supplemented with Con A (0.25 mg/ml), hyperosmotic sucrose (0.45M) or filipin (5 μg/ml) for 30 min before re-exposing the cells to QAPB (5 nM) in the continued presence of each individual inhibitor. QAPB intensity values were quantified by manually delimiting the profile of the fibroblast cells and averaging the QAPB fluorescence intensity within the delimited region of interest. All values of QAPB fluorescence intensity were corrected for background autofluorescence and the equilibrium QAPB intensity on this first exposure was normalized to 1. On a second exposure to QAPB, with or without test drugs, fluorescence intensity was measured at 30, 60 & 90 min and normalized to the "first

Molecular Pharmacology Fast Forward. Published on December 30, 2004 as DOI: 10.1124/mol.104.008417
This article has not been copyedited and formatted. The final version may differ from this version.



exposure" value. Normalized data from each experimental group was pooled and are presented as the mean ± s. e. mean. Statistical significance between the means was evaluated using a Student's paired *t*-test.

**Multiple fluorescent labeling of recycling and late endocytic vesicles.** R-1Fs seeded on to coverslips were rinsed with PBS and then exposed at room temperature to PBS containing either 10 nM QAPB and the recycling endosomal marker transferrin (Tfn)-Alexa Fluor$^{546}$, (20 μg/ml), or the late endosomal/lysomal marker Lysotracker Red-DND-99, (150 nM). Cells were pulse-labeled with Tfn Alexa Fluor$^{546}$ (37°C) or Lysotracker Red (room temperature) plus QAPB (10 nM) for 20 and 70 min respectively. At the end of each pulse labelling period, cells were then rinsed with PBS supplemented only with QAPB (10 nM) and then bathed in this solution for a further 15 min. Approximately 10 min before image acquisition, cells were exposed to PBS containing 10 nM QAPB plus the nuclear DNA-binding dye Hoechst 33342, (10 μg/ml, 10 min incubation at room temperature) to stain cell nuclei. Each coverslip was then washed and bathed in QAPB containing PBS before being imaged. The dyes Hoechst 33342, QAPB, Tfn Alexa Fluor$^{546}$ and Lysotracker Red were sequentially excited using the appropriate dichroics/filters to prevent bleedthrough and the resultant images were overlaid using MetaMorph software (version 6.2.6; Universal Imaging Corp., Downing, PA).

3D visualization of the co-localization of QAPB ligand-bovine $\alpha_{1a}$-AR complexes with Tfn Alexa Fluor$^{546}$ or Lysotracker Red was achieved by using a Nikon TE2000-E inverted microscope equipped with a z-axis linear encoded stepper motor. Each dye was sequentially excited and a z-series of images were acquired at 0.22-μm steps to produce individual z stacks. Z-stack images were then merged and deconvoluted using an iterative and constrained algorithm (Autodeblur software version 9.3.4**,** Autoquant Imaging, Watervliet, NY). Triplicate 3D (x-y, x-z and y-z) maximum projection views were constructed using Autovisualize software (Autoquant Imaging**,** Watervliet, NY).

**Fluorescence experiments undertaken in wild type and β-arrestin double knock out mouse embryo fibroblasts.** 24 hrs after transfection with the $\alpha_{1a}$-AR-EGFP2 fusion protein, cells were observed under oil immersion and fluorescence images were acquired at different time intervals in the absence or presence of the RQAPB ligand. During image acquisition, cells were maintained by superfusing them with HEPES-buffered saline solution. EGFP2 and RQAPB were excited using the

Molecular Pharmacology Fast Forward. Published on December 30, 2004 as DOI: 10.1124/mol.104.008417
This article has not been copyedited and formatted. The final version may differ from this version.



appropriate wavelength (490 nm for EGFP and 545 nm for RQAPB) and emitter (BP505-545 for EGFP and BP585-625 for RQAPB, (Chroma Technology). 3D-imaging was undertaken as previously described and 3D volumetric measurements of the proportion of surface EGFP2-tagged receptors binding RQAPB (relative to the total EGFP2-tagged $\alpha_{1a}$-ARs) was determined using Autodeblur software 9.3.4 (Autoquant Imaging, Watervliet, NY).

**Fluorescence experiments undertaken in HEK293T cells.**

**Dual Hoechst and QAPB epifluorescence imaging.** HEK293T cells transiently transfected with the non EGFP2-tagged version of the human $\alpha_{1a}$-AR were rinsed several times in PBS and then exposed to QAPB (10 nM) for 70 min at room temperature. Cell nuclei were stained prior to visualization. QAPB and Hoechst were sequentially excited and detected as previously detailed. Sequential images (no binning) were collected at 15 sec intervals.

**Dual EGFP2 and RQAPB confocal imaging**. Cells were plated on to glass coverslips (22 mm) and after a 24 h growth period they were transiently transfected with the EGFP2-tagged version of the human $\alpha_{1a}$-AR. Transfected cells were cultured overnight and 24 h later growth medium was removed and replaced with fresh PBS. Transfected cells were then pre-equilibrated with fresh PBS containing 10 nM of RQAPB, (a red fluorescent variant of the antagonist ligand QAPB), for 75 min. The RQAPB treated cells were mounted on to an imaging chamber and a Zeiss 510 PASCAL laser scanning confocal inverted microscope equipped with a 63 x oil immersion Plan Fluor Apochromat objective lens (NA=1.4) was used to visualize each fluorescent probe. Using the appropriate laser lines, (i.e. 488 nm for EGFP2 and 543 nm for RQAPB) and emission filters, (i.e. BP505-530 for EGFP2 and LP570 for RQAPB), sequential images were acquired to determine the total EGFP2 and RQAPB fluorescence emission intensity associated with each transfected cell. Overlay images were created as previously outlined.

**Solutions.** HEPES buffered saline solution contained (in mM) : NaCl, 130; KCl, 5; $CaCl_2$, 1; $MgCl_2$, 1; 4-(2-hydroxyethyl)-1-piperazine sulphonic acid (HEPES), 20; D-glucose, 10; pH adjusted to 7.4 using NaOH. Tris HCl assay buffer composition was: 150 mM NaCl, 50 mM Tris-HCl, 10 mM $MgCl_2$, 5 mM EDTA, pH 7.4.

Molecular Pharmacology Fast Forward. Published on December 30, 2004 as DOI: 10.1124/mol.104.008417
This article has not been copyedited and formatted. The final version may differ from this version.



# RESULTS

### Affinities of compounds measured by [$^3$H]-prazosin competition binding

Binding affinity estimates for the ligands used in this study were determined in R-1Fs stably expressing the bovine $\alpha_{1a}$-AR in order to set the quantitative context for visualization of ligand-ligand competition. Competition curves in membrane preparations between [$^3$H]-prazosin and both prazosin and its fluorescent analogue QAPB were monophasic and exhibited Hill coefficients that were close to unity, (Fig. 1). Prazosin and QAPB displayed subnanomolar affinity for the receptor. The $pK_i$ of phentolamine was 8.5 and this ligand was employed at high concentration (10 μM) to determine non-specific binding.

### Direct visualization of the fluorescent ligand-$\alpha_{1a}$-AR complex

#### Does fluorescent ligand binding coincide with receptors?

Non-transfected HEK293T cells showed no fluorescence on exposure to QAPB (10 nM) for 75 min (Fig. 2A [i] and [ii]). Similar exposure of cells transfected with the $\alpha_{1a}$-AR produced fluorescence predominantly in intracellular punctate vesicles, with a lower level reflecting cell surface localization (Fig. 2B). This is consistent with the concept that unbound QAPB does not fluoresce and that binding to the $\alpha_{1a}$-AR occurs with high affinity. In cells transfected with the $\alpha_{1a}$-AR-EGFP2 fusion protein, EGFP2 auto-fluorescence had a similar distribution (Fig. 2C [i]) to QAPB in $\alpha_{1a}$-AR (no EGFP2) cells (compare with Fig 2B). In the $\alpha_{1a}$-AR-EGFP2 expressing cells, exposure to the red version of QAPB produced red fluorescence (Fig. 2C [ii]) that co-localized with the green fluorescence of EGFP2 (Fig. 2C [iii]). This indicates that: (1) on incubation with live cells, QAPB binds to, and thus indicates the location of, all the $\alpha_{1a}$-AR population; (2) the ligand gains access to all compartments containing the EGFP2-labelled $\alpha_{1a}$-AR; (3) the receptor has affinity for the ligand at all of these sites (since unbound ligand does not fluoresce) (4) the EGFP2 tag does not alter receptor distribution or the movement of the organelles that they inhabit; (5) QAPB did not change the cellular disposition of EGFP2-tagged receptors, unlike agonists, which can cause a visible shift towards internalization. The similarity of the distribution of EGFP2 and QAPB also confirmed that the relative lack of cell surface QAPB binding is

Molecular Pharmacology Fast Forward. Published on December 30, 2004 as DOI: 10.1124/mol.104.008417
This article has not been copyedited and formatted. The final version may differ from this version.



an accurate reflection of the proportion of the receptor population at the plasma membrane rather than a technical artefact. As in HEK293T cells, QAPB labelling of the $\alpha_{1a}$-AR stably expressed in R-1F cells confirms the intracellular localization of the ligand/receptor complex in a second cell type. Data is presented as a 3D reconstruction (Fig. 2D, (i) x-y view, (ii) x-z view and (iii) y-z view, cell nuclei shown in blue and green punctate spots represent QAPB binding,).

Transiently transfected HEK293T cells were suitable for demonstrating features of cell distribution and co-localization but, because they had variable expression of the transfected receptors, they were less suitable for quantitative analysis of fluorescence ligand binding than stably transfected fibroblast lines.

**Time course of formation, spatial pattern and continuous movement of ligand-$\alpha_{1a}$-AR complexes.**

The equilibrated cells discussed above had indicated that QAPB gains access to all $\alpha_{1a}$-AR in live cells. The time course of the appearance (and disappearance) of fluorescence allowed analysis of the processes involved. Time-lapse epifluorescence images over 75 min were constructed in R-1F cells stably transfected with wild type receptor, and employing QAPB at a concentration (5nM) near its equilibrium constant (Fig. 3). Events were most easily seen and could be readily plotted by taking a 2-dimensional view that keeps the fluorescence from the whole cell thickness in the focal plane.

Within 1-2 min the cells were rapidly "covered" with ligand, as shown by low level diffuse fluorescence corresponding to binding to receptors on, or in close proximity to, the cell membrane (Fig. 3A [ii]). Slightly later, noticeable within 3-4 min of ligand application, higher intensity fluorescent signals appeared in punctate intracellular vesicles that were scattered throughout the cell cytoplasm (Fig. 3A [iii]). Very soon after this (5-10 min) higher intensity fluorescent signals started to appear in larger punctate structures near the nucleus (Fig. 3A [iv]) and their intensity increased steadily to equilibrium at 55-60 min (Fig. 3A [v]). The pattern of fluorescence therefore evolves from a small particulate distribution towards larger structures with time. Asterisk superimposed on image i of Fig. 3A represents the link to supplemental QuickTime movie 1, (created from assembled sequential time lapse images of image i over 75 min), which can be viewed at http://molpharm.aspetjournals.org.

Video sequence of movie 1 revealed that some of the fluorescent objects displayed short range bi-directional motion, whereas others were inert, or moved vast distances across the body of the R-1F.

Molecular Pharmacology Fast Forward. Published on December 30, 2004 as DOI: 10.1124/mol.104.008417
This article has not been copyedited and formatted. The final version may differ from this version.



Thus, the fluorescent organelles containing $\alpha_{1a}$-ARs moved continuously and this occurs in the absence of agonist stimulation.

This visual interpretation was confirmed quantitatively by binning the pixels according to their intensity (Fig. 3C) and then displaying the contents of each bin as a time course (Fig. 4A). In this way the binding to receptors over the whole cell surface can be distinguished from binding to the punctate intracellular structures, which represent a smaller fraction of the image but are brighter. The lowest intensity bin (Bin 1), which contains the black pixels and the background fluorescence, is omitted from the graphs. Bin 2 is the lowest intensity bin that shows specific fluorescence. This shows the rapid acquisition of the binding signal over the whole cell surface. It reached a peak at between 2 and 3 min and, at this time, there were no high intensity signals because it was too early for the ligand to have reached the intracellular structures. However, after 3 min the higher intensity bins started to increase in sequence as the punctuate intracellular structures appeared. A consequence of this was that the number of pixels in Bin 2 decreased as the punctuate structures took over their pixels. The time course of the increase in the number of pixels in the highest intensity bins indicates the slower acquisition of binding by the intracellular structures until ligand binding reached a steady-state (at 40-60 min; Fig 3A, image v; Fig. 4A). Note that the total number of pixels in the "brighter bins" (Bins 3-8) remained constant after 10 min but the number in the brightest bins (Bins 5-8) increased at the expense of the intermediate bins (Bins 3 and 4), i.e. all the intracellular structures were fully revealed at 10 min but they did not become saturated until 60 min.

**Separation of $\alpha_{1a}$-ARs in intracellular pools and at the cell surface in R-1Fs**

Receptor expression on the cell surface can be estimated from the rapid, initial, diffuse binding that occurs after addition of ligand but before the intracellular organelles can be visually resolved. This occurred within 2 min, (Fig. 3A [ii]), indicating a rapid association rate for the ligand and surface-located receptors. The sum of the cellular fluorescence at this point in time thus represents the total of the cell surface receptors. When equilibrium occurs, in a 2D image that visualises everything in the cell, the image of the intracellular binding is superimposed upon this surface image. Subtraction of this image from the equilibrium image thus leaves the image of the intracellular binding (Fig. 3B). Since the surface image is constant, this subtraction can be applied to a time series of images to leave a much

Molecular Pharmacology Fast Forward. Published on December 30, 2004 as DOI: 10.1124/mol.104.008417
This article has not been copyedited and formatted. The final version may differ from this version.



enhanced view of the mobile intracellular organelles (Fig. 3B) and proved a remarkably effective way of separating the images of the surface and intracellular ligand-receptor complex.

This information could then be used quantitatively to assess relative numbers of receptors on the surface and inside cells. Since the fluorescence at equilibrium represents the total receptor population, the proportion of receptors on the surface can be calculated from the ratio of binding at 2 min and at equilibrium, giving a surface population of 30% and intracellular of 70%. When the surface binding was subtracted from the binding at each time point a graph of the rate of binding detected in intracellular sites could be constructed (Fig. 4C; compare solid black line with broken line trace). From this graph a rate constant for the appearance of intracellular binding could be estimated. The resulting $t_{1/2}$, of 12.4 min did not differ significantly from the equivalent value calculated from the total fluorescence, i.e. 12.5 min (Table 2).

**Reversal of binding by washing or the competitive antagonist phentolamine**

*Washout:* The binding of QAPB was reversible when the ligand was withdrawn from the superfusate (Figs. 3D and 5B). Viewing the time lapse or movie showed a steady fade of all parts of the image but was less easy to analyse visually, than the "on" phase. Quantitative analysis showed essentially a reversal of the histogram intensity pattern compared with the "on" phase (a progressive shift towards lower intensity bins), (Fig. 4B). However, in contrast to the fast initial increase in low intensity pixels in the "on" phase binding, the initial event was a slow but steady fall in the number of pixels across the high intensity bins suggesting that outgoing receptor-ligand complexes were replaced by vacant receptors (there is a corresponding increase in the number of low intensity pixels in Bin 2 as the punctate structures disappear). While this is not dramatic on the histogram plot, because these pixels are of high intensity, the fall in overall fluorescence was substantial and rapid (Fig. 5B). The overall pattern was therefore of loss from the inside, with low intensity surface binding last to disappear, as would be expected if ligand-receptor complexes steadily returned to the surface.

*Phentolamine:* Although washing with saline produced a rapid fall in QAPB fluorescence, the $t_{1/2}$ for the disappearance of fluorescence, 22.0 min (Table 2 and Fig. 5B) was slower than for its appearance. This could be accounted for by re-association of ligand since washing in the presence of an excess of phentolamine (100 μM; n=3) increased the rate of loss of QAPB fluorescence by a factor of 2; $t_{1/2}$, 10.7

Molecular Pharmacology Fast Forward. Published on December 30, 2004 as DOI: 10.1124/mol.104.008417
This article has not been copyedited and formatted. The final version may differ from this version.



min (Table 2 and Fig. 5B, pooled data points; dark grey line). Thus the true rates of uptake and loss are very similar, at 12.5 and 10.7 min, respectively.

Phentolamine was able to displace fluorescent ligand even in the continued presence of QAPB (5 nM) in the saline. This was concentration-dependent (Fig. 5): At 10 μM phentolamine was not fully effective (Fig. 5A, image [iii]), but 100 μM was, (Fig. 5A [iv] & 5B), thus establishing that all detectable binding was specific and that the fluorescent receptor-ligand complexes were susceptible to competitive ligands. Displacement in the continued presence of QAPB by phentolamine (100 μM) was slower than washing with or without phentolamine (Table 2 and Fig. 5B, light grey line, $t_{1/2}$, 25.6 min, n=4, as expected if some bound ligand continued to be internalized before equilibration with phentolamine had been attained.

**Estimation of receptor cycling time and residence at cell surface**

If the receptor population is spontaneously cycling, the average time at the surface should be the same proportion of the total cycling time. The cycling time cannot be calculated accurately from this data but its limits can. Since half-saturation is achieved in 12.5 min (Table 2) it is a reasonable working assumption that one inward leg of the cycle must occur within this time even if all receptors carried a bound ligand molecule (and the equilibrium binding data suggests that there would be of the order of 90% saturation, provided that the receptors were located at the surface long enough to equilibrate). This is supported by the rate of loss of fluorescence when the ligand was withdrawn in an excess of competitor, which was very similar; $t_{1/2}$ 10.7 min (Table 2). Together these data allow the estimate that a full cycle is less than 25 min. Therefore, the average residence at the cell surface should be less than 7.5 min (30% x 25 min).

**Is endocytosis involved in internalization of ligand?**

The hypothesis that the QAPB ligand is internalized in association with recycling receptors was validated by blocking clathrin-coated pit/vesicle formation endocytosis using either Con A or hypertonic sucrose (Fonseca *et al*., 1995). It was first shown, quantitatively, that QAPB binding was reversible and reproducible (Fig. 6, open bars). Con A (0.25 mg/ml) or hyperosmotic sucrose (0.45 M),

Molecular Pharmacology Fast Forward. Published on December 30, 2004 as DOI: 10.1124/mol.104.008417
This article has not been copyedited and formatted. The final version may differ from this version.



significantly inhibit the binding of QAPB (Fig. 6 black and grey bars) to recycling $\alpha_{1a}$-ARs. After 30 min exposure to Con A or sucrose, QAPB fluorescence was inhibited by 84 ± 6% ($p<0.001$, n=5) and 85 ± 3% ($p<0.001$, n=5), respectively. This inhibition was maintained over 90 min with only a small further accumulation of fluorescence (Fig. 6). Filipin (5 μg/ml), an inhibitor of caveolar endocytosis, had no effect at any time point (shown at 90 min in fig 6B, dotted black bar).

**Is β-arrestin necessary for the internalization or trafficking of $\alpha_{1a}$-ARs ?**

This was tested in MEFs devoid of β-arrestin 1/2. The $\alpha_{1a}$-AR-EGFP2 fusion protein was predominantly expressed inside these cells in a clumped and clustered vesicular arrangement (Fig. 7A, images i and ii, green colour, white arrows) that presumably reflects the well appreciated limitation of many transiently transfected cells to effectively mature and deliver receptors to the cell surface.

Asterisk on image i of Fig. 7A represents the link to movie 2 prepared from assembled images of image i recorded at 15 sec intervals. Video sequence of movie 2 indicated that the intracellular, clumped pool of $\alpha_{1a}$-AR-EGFP2 was motionless, in contrast with observations in wild type MEF cells (see later). Despite this, in both sets of MEF cells some of the $\alpha_{1a}$-AR-EGFP2 fusion protein was localized at the cell surface (Fig. 7A, [i] and [ii], green colour, red arrows). In the β-arrestin 1/2 deficient cells, after 75 min exposure to RQAPB (10 nM) the intracellular $\alpha_{1a}$-AR-EGFP2 had not bound the RQAPB ligand, (Fig. 7B, overlay image iv, white arrows). RQAPB did bind on the cell surface, where it co-localized with EGFP2-labelled surface $\alpha_{1a}$-ARs (Fig. 7B, image iv, red arrow, yellow represents co-localization). Asterisk on top of overlay image iv of Fig. 7B represents the link to movie 3 showing a 3D y-z view of this image. Movie 3 clearly indicates the RQAPB ligand-$\alpha_{1a}$-AR–EGFP2 complex (yellow) only on the surface of the MEF cell. The volume of $\alpha_{1a}$-AR-EGFP2, (surface plus intracellular) and RQAPB labelled $\alpha_{1a}$-AR-EGFP2 complex, (surface only), was 1823 and 1232 $\mu M^3$ respectively. The volume of intracellular EGFP2-tagged $\alpha_{1a}$-ARs not labelled with RQAPB was 590 $\mu M^3$, (i.e. 32% of the total available EGFP2-tagged receptors). The relative fraction of surface to intracellular $\alpha_{1a}$-ARs, (at steady-state), was 68% and 32% respectively. This indicates that RQAPB did not gain access to the intracellular pool of $\alpha_{1a}$-ARs in β-arrestin negative MEF cells, demonstrating further that the ligand is not able to diffuse efficiently across the cell surface. By contrast, in wild type MEF cells that express

Molecular Pharmacology Fast Forward. Published on December 30, 2004 as DOI: 10.1124/mol.104.008417
This article has not been copyedited and formatted. The final version may differ from this version.



β-arrestins the $\alpha_{1a}$-AR-EGFP2 recycled, (movie not shown), and after pre-equilibration with RQAPB (10 nM) for 75 min, it was observed that the RQAPB ligand co-localized with both cell surface (red arrow) and intracellular (white arrow) EGFP2-tagged $\alpha_{1a}$-ARs (Fig. 7C, overlay image iv, yellow represents co-localization). Asterisk on overlay image iv of panel C of Fig. 7 represents the link to movie 4 showing a 3D y-z view of this image. The video sequence of movie 4 clearly shows the RQAPB ligand-$\alpha_{1a}$-AR–EGFP2 complex (yellow) inside and on the cell surface. As anticipated from the above, non-transfected wild type MEFs displayed no RQAPB fluorescence after 75 min exposure (Fig. 7C, compare image i with ii and iii.). These studies also support the hypothesis that RQAPB has to bind to cell surface receptors prior to its internalization and entry into the cell.

**Are $\alpha_{1a}$-AR-and β-arrestin-found together?**

To answer this, R-1F cells were employed that expressed both β-arrestin 2-EGFP and the bovine $\alpha_{1a}$-AR. This resulted in non-uniform cytoplasmic localization of β-arrestin 2-EGFP with more intense β-arrestin-2-related fluorescence expressed in punctate vesicles (Fig 8A, image i, green vesicles some shown by white arrows). In contrast to this pattern, introduction of β-arrestin 2-EGFP into otherwise non-transfected R-1Fs resulted in a uniform cytoplasmic distribution of the tagged β-arrestin 2 (data not shown). Asterisk overlayed on image i of Fig. 8A represents the link to movie 5 prepared from reconstructed sequential time lapse 2D-images of image i recorded at 15 sec intervals. Movie 5 revealed that the organelles containing β-arrestin 2-EGFP showed rapid movement around the cells similar to that found for organelles carrying $\alpha_{1a}$-ARs (movie 5; Fig. 8A, image i). No significant change in the localization or movement of β-arrestin 2-EGFP2 occurred upon exposure, (15 min), to the agonist phenylephrine, (PE), (3 μM), (Fig. 8A, compare image ii with iii). The same was found for the antagonist/inverse agonists prazosin, (3 μM), phentolamine (3 μM) and RQAPB (10 nM), (data not shown).

When $\alpha_{1a}$-ARs were labelled with RQAPB (10 nM), it partly co-localized with β-arrestin 2-EGFP, (Fig. 8B, image iv); yellow/orange punctate vesicles, some illustrated by white arrows). The degree of co-localization was quantified by plotting the amount of background-subtracted green EGFP fluorescence from the pixels in a region of interest, (see Fig. 8C, red rectangle superimposed on image

Molecular Pharmacology Fast Forward. Published on December 30, 2004 as DOI: 10.1124/mol.104.008417
This article has not been copyedited and formatted. The final version may differ from this version.



ii and iii), against the amount of back-ground red fluorescence in the corresponding pixels of the matched region in the RQAPB image. Correlation coefficients were quantified that described the degree by which EGFP and RQAPB fluorescence at each pixel within the region varied from a perfect correlation of 1.00. Calculated correlation coefficient was 0.91 indicating that RQAPB-labelled bovine $\alpha_{1a}$-ARs co-localized very efficiently with β-arrestin-2-EGFP. Collectively, these data demonstrate partial, spontaneous association of $\alpha_{1a}$-AR with β-arrestin-2EGFP- and indicate that $\alpha_{1a}$-AR recycling is a β-arrestin-dependent, ligand-independent process.

**Which endosomal compartments does the ligand-$\alpha_{1a}$-AR complex enter?**

To visualize and determine the identity of the intracellular compartments where the QAPB-receptor complexes resided, we examined potential co-localization with fluorescent reagents that can selectively identify different subcellular compartments. Tfn Alexa Fluor$^{546}$, a recycling endosome fluorescent marker for endocytosis via clathrin-coated pits (Anderson, 1998; Gagnon *et al.*,1998) was used to identify the recycling pathway. Merged images, presented in Fig. 9A, image iii, show that after 40 min, fluorescence corresponding to $\alpha_{1a}$-AR-QAPB ligand sites (green punctates, Fig. 9A, image i) partially overlapped with the fluorescent recycling marker (yellow perinuclear vesicles, some indicated by white arrows, Fig. 9C, image iii). A proportion of the receptor-QAPB ligand binding sites was spatially distinct from the recycling endosomal Tfn receptors (Fig. 9C, image ii, red punctates). A 3D x-z view of bovine $\alpha_{1a}$-AR-QAPB ligand complexes partially co-localizing with recycling compartments (yellow punctates, white arrows) is shown in image iv of Fig. 9A.

Lysotracker Red DND-99, a highly selective red fluorescent acidotrophic probe for labelling acidic organelles (Bucci *et al*., 2000), was used to identify acidic late endosomes. After 90 min, Lysotracker Red fluorescence had extensive overlap with the intracellular structures binding QAPB (Fig. 9B, image iii, yellow punctates, some shown by white arrows, compare images i, ii and iii in panel B of Fig. 9), implying that $\alpha_{1a}$-AR ligand complexes were trafficked to the late endosomal/lysomal network. 3D x-z co-localization view of bovine $\alpha_{1a}$-AR-QAPB ligand complexes fusing with late/lytic endosomes is shown in Fig. 9B, image iv (yellow punctates, white arrows).

Molecular Pharmacology Fast Forward. Published on December 30, 2004 as DOI: 10.1124/mol.104.008417
This article has not been copyedited and formatted. The final version may differ from this version.



**DISCUSSION**

Visualizing the receptor/ligand complex in real-time demonstrates that the $\alpha_{1a}$-AR is spontaneously internalized by endocytosis when expressed in a range of cells including R-1Fs. The receptor continuously recycles, spending a relatively small fraction of time at the cell surface. Most of the time each receptor molecule is present in intracellular organelles that shuttle between the cell surface and perinuclear compartments, including early and late endosomes. Both receptor internalization and the formation and movement of the mobile intracellular organelles are dependent on β-arrestins but not on receptor activation.

Cycling is continuous and rapid, with complete turnover within 50-60 min. This has implications for understanding the "purpose" and properties of recycling and the dynamics of drugs acting at the receptors. The rate of agonist-induced internalization is not known in the case of $\alpha_{1a}$-AR but it is more resistant to desensitization than $\alpha_{1b}$-AR (Vazquez-Prado *et al*., 2000). Agonist-induced internalization, as judged by disappearance of cell surface receptors, is undetectable for tagged $\alpha_{1a}$-ARs in R-1Fs after 10 min (Price *et al.*, 2002) and achieves small reductions even after 60 min of high concentrations of agonists (Morris *et al*., 2004; Stanasila et al, 2003). These net shifts of location may of course disguise an increase in recycling, with only the net shift in location being detected. Thus, constitutive recycling is the phenomenon more likely to occur in physiological conditions.

Agonist-induced recycling of $\alpha_1$-AR has yet to be demonstrated at physiological concentrations of natural agonists or in native cells. When the $\alpha_{1a}$-AR is localized in native cells such as smooth muscle or hepatocytes it has consistently shown a predominant intracellular location coupled with a less dominant plasmalemmal location (Mackenzie *et al*., 1998; McGrath *et al*., 1999; Hrometz *et al*, 1999; Mackenzie *et al*., 2000; Deighan *et al*., 2004; Miquel *et al*., in press; reviewed in Daly & McGrath, 2003). This could result from modulation by low levels of physiological agonist activation. Spontaneous $\alpha_{1a}$-AR recycling may maintain an internal reserve pool of receptors that can sustain continuous agonist-induced signalling in the face of stimulation-induced attrition of the surface population, as suggested by Morris *et al.,* (2004).

Our current advance is the ability to visualize and follow the receptor/ligand complex in real-time. EGFP2-tagged receptors show total receptor localization but provide no information on movement within this population. Fluorescent antagonist ligands show the most recently labelled receptors that

have internalized. Ligands access the interior of cells only if bound to endocytosing receptors since ligands enter only cells that possess both the receptor and β-arrestins.

The rate of appearance of intracellular fluorescence provides a time and concentration profile of the internalizing receptors from which rates of entry and of receptor recycling turnover can be estimated. This is analogous to the established use of antibodies to extracellular epitope tags for the study of internalization (e.g. Morris *et al*., 2004) but, additionally, can be followed in real-time and, in conjunction with other vital dyes, can provide information on coincident dynamic events. The entire population recycles within 25 min so the average residence time of the 30% at the cell surface is less than 7.5 min, even without stimulation.

The rapidity of these events has implications for receptor signalling and regulation. It cannot be assumed that internalized receptors are in a desensitized state that is incapable of signalling, although interaction with a β-arrestin will prevent concurrent interaction with G protein. An emerging literature indicates a distinct set of signalling functions for β-arrestins, particularly in the regulation of the kinetics and effectiveness of MAP kinase signalling cascades (Shenoy and Lefkowitz, 2003, Lefkowitz and Whalen, 2004). Although receptors are able to internalize with agonists bound, the low pH of recycling and other endosomes encourages dissociation and it is likely that only high affinity agonist ligands, e.g. peptides, remain bound throughout the cycle. Equally, the paradigm of agonist-mediated internalization may require modification since agonists may simply accelerate spontaneous endocytosis rather than initiate it. A change in the balance of surface:intracellular receptors will occur only when the inward rate exceeds the rate of return to the surface and this concept can be modelled mathematically (Koenig and Edwardson, 1997, Koenig, 2004).

Real time visualization of movement of endosomal ligand-receptor complexes can allow the study of recycling in native cells, until now, impractical due to the need for epitope tags. Receptors in mobile endosomes have been visualized previously only by using GFP-tagged GPCRs (Kallal and Benovic, 2002; Koenig and Edwardson, 1997). Since an identical pattern of distribution and movement is found with the ligand or EGFP, their co-localization provides cross-validation of both techniques. Neither the EGFP2 tag nor the bound ligand slows endosomal movement or changes receptor distribution.

In cells devoid of β-arrestins, immobility of EGFP2-tagged receptor showed that β-arrestins are needed for the genesis of the mobile endosomes, a key part of the recycling system. Without them,

Molecular Pharmacology Fast Forward. Published on December 30, 2004 as DOI: 10.1124/mol.104.008417
This article has not been copyedited and formatted. The final version may differ from this version.



receptors remained immobile in a fixed reticular endosomal compartment. Nevertheless, the proportion of receptors at the surface in β-arrestin-deficient MEF cells was similar to wild type MEF cells so β-arrestins are necessary for recycling but recycling does not regulate partitioning of the receptor population.

Vesicles containing ligand-receptor complexes moved to and from the plasma membrane, indicating a ferrying function. This was visible for QAPB-labelled receptors in both R-1Fs and HEK293T cells and for EGFP2-labelled receptor in HEK293T cells. These movements are therefore an inherent property of the cells and not a phenomenon instigated by receptor occupation or cell type. The development with time of the intensity of these fluorescent structures when the cells were exposed to QAPB, is akin to development of a photograph. Before uncovering the key role of endocytosis it might have been assumed that ligand diffused into the cell, where it bound to internally located, immobile receptors. Internalization of QAPB can now be understood in terms of endocytosis of a QAPB-receptor complex. In endocytosis the basic units of transport are small structures, beyond the resolution of the microscope, e.g. caveoli or endocytic vesicles, that reversibly fuse with small visible structures to exchange a cargo of plasma proteins including the ligand-receptor complex. These small fluorescent "transit" endosomes then move further into the cell and reversibly fuse with larger perinuclear endosomes, delivering ligand-receptor complexes.

Movements of transit vesicles and their transactions with the perinuclear complexes are made visible by the high concentrations of receptor-ligand complexes on their resolvable surfaces. The intensity per pixel shows receptor density to be 5 times higher than on the cell surface indicating a high degree of physical marshalling and cargo selection. In all these intracellular transactions the ligand and binding site are restricted to the internal face of endosomes so that, even if they dissociate, the ligand molecules will be restricted to the compartment and likely to re-associate. QAPB leaves the cell again on its removal from the extracellular environment, with a time course similar to its endocytic uptake, so it seems likely that it leaves the cell by the reverse process, bound to receptors recycling back to the cell surface.

Many $\alpha_1$-AR antagonists are inverse agonists, including the quinazolyl-piperazine (e.g. prazosin, doxazosin, alfuzosin) family to which QAPB belongs (García-Sáinz and Torres-Padilla, 1999; Price *et al*., 2002). However, the wild type $\alpha_{1a}$-AR receptor has low levels of constitutive activity (Price *et al*.,

2002; Rossier *et al*., 1999). Furthermore, antagonists including prazosin and QAPB do not produce either a depression or a rise of resting $[Ca^{2+}]_i$ in these R-1F cells (Pediani *et al*., 2000) eliminating inverse agonism and partial agonism. Additionally, Morris *et al*., (2004) showed that prazosin did not affect spontaneous endocytosis of the HA-tagged $\alpha_{1a}$-AR and our data with phentolamine is consistent with competition and displacement of QAPB rather than blockade of recycling.

Endocytosis was established as the entry mechanism for ligand/receptor complex using two independent agents (hyperosmotic sucrose, Con A), that block clathrin-mediated internalization (Daukas and Zigmond, 1985; Heuser and Anderson, 1989) and involvement of β-arrestins was confirmed by the absence of ligand uptake in β-arrestin-deficient MEF cells and by the partial co-localization of β-arrestin-2-GFP with the ligand/receptor. The generalisation that interactions between receptor and β-arrestins require agonist-mediated phosphorylation of the receptor no longer holds. Such phosphorylation frequently increases the affinity of such interactions rather than defining them. For example, interactions between β-arrestins and the protease activated receptor-1 is independent of receptor phosphorylation (Chen *et al.,* 2004) as are such interactions with the BLT1 leukotriene $B_4$ receptor (Jala *et al*., 2004). However, the interactions of β-arrestins with components of the machinery of clathrin-mediated endocytosis are central to the delivery of β-arrestin/receptor complexes to clathrin-coated pits (Ferguson *et al*., 1996). Filipin, an inhibitor of caveolar endocytosis, had no major effect on uptake of QAPB. These results show that endocytosis via clathrin-coated vesicles is responsible for the ingress of QAPB.

The receptors initially enter in a similar manner as Tfn and after a longer period penetrate endocytotic compartments beyond the limit of Tfn's ingress. Here they are trafficked to more acidic vesicles: in the late endosomes, the receptors then go through a second stage of sorting and either are targeted to lysosomes for degradation or are slowly recycled back to the cell surface (Mellman, 1996; Resat *et al*., 2003). Their dynamic equilibrium prevents easy distinction between early, late and lysosome compartments so we cannot estimate their relative proportions or the amount of receptor degradation. However, saline washing eliminated fluorescent ligand from cells excluding accumulation in a compartment for long term storage. A high proportion of the receptors was found in endocytic vesicles in both cells types employed. This might be attributed to "overexpression" in these recombinant systems but it is very similar to native systems such as smooth muscle cells from rat blood

vessels and human prostate that express $\alpha_1$-ARs (Mackenzie *et al*., 1998, 2000; McGrath *et al*., 1999; Deighan *et al*., 2004).

Spontaneous endocytosis responsible for internalization of the $\alpha_{1a}$-AR and its antagonist ligand cargo, is a new paradigm for uptake of antagonist drugs. It alters the potential mechanisms involved when whole cells are used in radioligand binding assay. Order of addition of drugs to cells becomes a potential source of variability, and time to equilibrium should be longer than if all binding were on the cell surface. When "membrane" preparations are used, many receptors will derive from intracellular membranes and this may influence their properties given the greater densities and the presence of different co-factors. Based on susceptibility to internalization, receptors are categorised into those that internalize/recycle constitutively or upon binding agonist (Milligan and Bond, 1997). However receptors internalizing with antagonists attached do not fit this scheme. Agonist-independent GPCR internalization has been observed for the angiotensin $AT_{1A}R$ and cholecystokinin receptors (Anborgh *et al*., 2000; Hein *et al*., 1997; Tarasova *et al.,* 1997). For angiotensin $AT_{1A}R$, β-arrestin association with receptor, without agonist, is responsible for agonist-independent loss of cell surface receptor (Anborgh *et al*., 2000). The $\alpha_{1a}$-AR can now be added to the "spontaneously recycling", β-arrestin-dependent category. How widely this applies amongst other GPCTR remains to be seen. The cellular uptake of α-blockers at low concentrations also introduces a new concept into their mechanism of action in treating conditions such as benign prostatic hyperplasia. Intracellular concentration of drug at receptor-dense sites raises potential intracellular actions that require investigation and introduces new pharmacokinetic issues.

In conclusion, $\alpha_{1a}$-AR recycle rapidly by agonist-independent, constitutive, β-arrestin-dependent processes. Receptors spend most of their time in endosomal recycling compartments, and have a relatively short residence at the cell surface. Antagonists that bind to the receptive site are internalized with the receptor and transported through the recycling process, attaining saturation binding to intracellular receptors.

Molecular Pharmacology Fast Forward. Published on December 30, 2004 as DOI: 10.1124/mol.104.008417
This article has not been copyedited and formatted. The final version may differ from this version.



**ACKNOWLEDGEMENTS**

DC was supported by an MRC PhD studentship and JFC by the Ann B McNaught Bequest. The authors thank Professor Gwyn Gould (IBLS, Biochemistry and Molecular Biology, University of Glasgow) for helpful discussions.

**REFERENCES**

Anborgh, P.H., Seachrist, J.L., Dale, L.B. and Ferguson, S.S.G. (2000). Receptor/beta arrestin complex formation and the differential trafficking and resensitisation of beta-2-adrenergic and angiotensin II type 1A receptors. *Mol. Endocrinol*, **14**:2040-2053.

Anderson, R.G. (1998). The caveolae membrane system. *Annu Rev Biochem*, **67**:199-225.

Bucci, C., Thomsen, P., Nicoziani, P., McCarthy, J. and van Deurs, D. (2000). Rab7: A key to lysosome biogenesis. *Mol Biol Cell,* **11**:467-480.

Chen CH, Paing MM, Trejo J. (2004) Termination of protease-activated receptor-1 signaling by beta-arrestins is independent of receptor phosphorylation. *J. Biol. Chem*. **279**: 10020-10031.

Cheng, Y.C. and Prusoff, W.H (1973). Relationship between the inhibitor constant ($K_i$) and the concentration of inhibitor which causes 50 percent inhibition of an enzymatic reaction. *Biochem Pharmacol Med,* **22**:3099-3108.

Daly, C.J. and McGrath, J.C. (2003). Fluorescent ligands, antibodies and proteins for the study of receptors. *Pharmacology & Therapeutics*, **100**:101-118.

Daly, C.J., Milligan, C.M., Milligan, G., Mackenzie, J.F. and McGrath, J.C. (1998). Cellular localisation and pharmacological characterisation of functioning $\alpha_1$-adrenoceptors by fluorescent ligand binding and image analysis reveals identical binding properties of clustered and diffuse populations of receptors.*J. Pharmacol. Exp. Ther*, **286**:984-990.

Daukas, G. and Zigmond, S.H., (1985). Inhibition of receptor-mediated but not fluid phase endocytosis in polymorphonuclear leucocytes.*J. Cell Biology,* **101**:1673-1679.

Deighan, C., Woollhead, A.M., Colston, J.F., McGrath, J.C. (2004). Hepatocytes from $\alpha_{1B}$-adrenoceptor knockout mice reveal compensatory adrenoceptor subtype substitution. *British Journal of Pharmacology,* **142**:1031-1037

Ferguson, S.S.G., Downey, W.E., Colapietro, A..M., Barak, L.S., Menard, L. and Caron, M. (1996). Role of β-arrestin in mediating agonist-promoted G protein-coupled receptor internalization. *Science,* **271**:363-366.

Fonseca, M.I., Button, D.C. and Brown, R.D. (1995). Agonist regulation of $\alpha_{1b}$-ARs-adrenergic receptor subcellular distribution and function. *J Biol Chem*, **270**:8902-8909.

Gagnon, A.W., Kallal, L. and Benovic, J.L. (1998). Role of clathrin-mediated endocytosis in agonist induced downregulation of the beta-2-adrenergic receptor. *J Biol Chem*, **273**:6976-6981.

García-Sáinz, J. A.. and Torres-Padilla, M. E. (1999). Modulation of basal intracellular calcium by inverse agonists and phorbol myristate in rat-1 fibroblasts stably expressing $\alpha_{1d}$-adrenoceptors. *FEBS Lett,* **443**:277-281.

Hein, L. Meinel, L., Pratt, R.E., Dzau, V.J. and Kobilka, B.K. (1997). Intracellular trafficking of angiotensin II and its $AT_1$ and $AT_{1I}$ receptor: evidence for selective sorting of receptors and ligand. *Mol. Endocrinol,* **11**:1266-1277.

Heuser, J.E. and Anderson, R.G. (1989). Hypertonic media and Concanavalin A inhibit receptor-mediated endocytosis by blocking clathrin coated pit formation. *J. Cell Biol*, **108**:389-400.

Hrometz, S.L, Edelmann, S.E, McCune, D.F, Olges, J.R, Hadley, R.W., Perez, D.M., and Piascik, M.T. (1999). Expression of multiple $\alpha_1$-adrenoceptors on vascular smooth muscle: correlation with the regulation of contraction. *J Pharmacol Exp Ther*, **290:** 452-463.

Jala VR, Shao WH, Haribabu B. (2004) Phosphorylation Independent beta -arrestin translocation and internalization of leukotriene B4 receptors. *J. Biol. Chem*. [Epub ahead of print] Nov 23 PMID: 15561704

Kallal, L. and Benovic, J.L. (2000). Using green fluorescent proteins to study G-protein-coupled receptor localisation and trafficking. *Trends Pharmacol. Sci*, **21**:175-180.

Kallal, L. and Benovic, J.L. (2002). Fluorescent microscopy techniques for the study of G-protein-coupled receptor trafficking. *Methods Enzymol,* **343**:492-506.

Koenig, J.A. (2004) Assessment of receptor internalization and recycling. *Methods Mol. Biol*. **259**:249-273.

Koenig, J.A. and Edwardson, J.M. (1997). Endocytosis and recycling of G protein-coupled receptors. *Trends Pharmacol. Sci,* **18**:276-287.

Kohout, T.A., Lin, F-T, Perry, S.J., Conner, D.A. and Lefkowitz, R.J. (2001). β-arrestin 1 and 2 differentially regulate heptahelical receptor signaling and trafficking*, PNAS*, **98**:1601-1606.

Lefkowitz, R.J. and, Whalen, E.J. (2004) beta-arrestins: traffic cops of cell signaling. *Curr. Opin. Cell Biol*. **16**:162-168.

Mackenzie J.F., Daly, C.J., Pediani, J.D. and McGrath, J.C. (2000). Quantitative imaging in live human cells reveals intracellular alpha1-adrenoceptor ligand-binding sites. *J Pharmacol Exp Ther*, **294**:434-443.

Mackenzie, J.F., Daly, C.J., Luo, D. & McGrath, J.C. (1998). Cellular localisation of alpha-1 adrenoceptors in native smooth muscle cells. On-line Proceedings of the 5th Internet World Congress on Biomedical Sciences '98 at McMaster University, Canada (download from URL: http://www. .mcmaster.ca/inabis98/cvdisease/mackenzie089/index.html)

McGrath, J.C., Arribas, S.M. and Daly, C.J. (1996). Fluorescent ligands for the study of receptors. *Trends Pharmacol. Sci,* **17**:393-399.

McGrath, J.C., Mackenzie, J.F. and Daly, C.J. (1999). Pharmacological implications of cellular localization of alpha1-adrenoceptors in native smooth muscle cells, *J Auton Pharmacol*, **19**:303-310.

Mellman, I. (1996). Endocytosis and molecular sorting. *Annu. Rev. Cell Dev. Biol,* **12**:575-625.

Milligan, G. and Bond, R.A. (1997). Inverse agonism and the regulation of receptor number. *Trends Pharmacol. Sci,* **18**:468-474.

Miquel, M.R., Segura, V, Ali, Z., D'Ocon, M. P., McGrath, J.C. and Daly, C.J. (2004). 3D image analysis of fluorescent drug binding. Molecular Imaging, MIT Press, accepted 12th November 2004, (in press).

Morris, D.P., Price, R.R., Smith, M.P., Lei, B. and Schwinn, D.A. (2004). Cellular Trafficking of Human $\alpha_{1a}$-adrenergic receptors is continuous and primarily agonist-independent. *Mol Pharmacol*, **66**:843-854.

Pediani, J.D., MacKenzie, J.F., Heeley, R.P., Daly, C.J. and McGrath, J.C. (2000). Single-cell recombinant pharmacology: bovine $\alpha_{1a}$-adrenoceptors in rat-1 fibroblasts release intracellular $Ca^{2+}$, display subtype-characteristic agonism and antagonism, and exhibit an antagonist-reversible inverse concentration-response phase. *J Pharmacol Exp Ther*, **293**:887-895.

Price, R.R., Morris, D.P., Biswas, G., Smith, M. P. and Schwinn, D. A. (2002). Acute agonist-mediated desensitization of the human $\alpha_{1a}$-adrenergic receptor is primarily independent of carboxyl terminus regulation : implications for regulation of $\alpha_{1a}$-AR splice variants. *J. Biol. Chem,* **277**:9570-9579.

Resat, H., Ewald, J.A., Dixon, D.A. and Wiley, S.H (2003). An integrated model of epidermal growth factor receptor trafficking and signal transduction. *Biophysical Journal*, **85**:730-743.

Rossier, O., Abuin, L., Fanelli, F., Leonardi, A. and Cotecchia, S. (1999). Inverse agonism and neutral antagonism at alpha (1a)- and alpha (1b)-adrenergic receptor subtypes. *Mol Pharmacol*, **56**:858-866.

Roettger BF, Ghanekar D, Rao R, Toledo C, Yingling J, Pinon D, Miller LJ (1997) Antagonist-stimulated internalization of the G protein-coupled cholecystokinin receptor *Mol. Pharmacol* **51**:357-362.

Shenoy SK, Lefkowitz RJ. (2003) Multifaceted roles of beta-arrestins in the regulation of seven-membrane-spanning receptor trafficking and signalling. *Biochem. J.* **375**:503-515.

Stanasila, L., Perez, J.B., Vogel, H., Cotecchia, S. (2003). Oligomerization of the alpha 1a- and alpha 1b-adrenergic receptor subtypes. Potential implications in receptor internalization. *J Biol Chem*, **278**:40239-40251.

Tarasova, N.I., Stauber, R.H., Choi, J. K., Hudson, E.A., Czerwinski, G., Miller, J.L., Pavlakis, G.N., Michejda, C.J. and Wank, S.A. (1997). Visualisation of G-protein-coupled receptor trafficking with the aid of the green fluorescent protein. Endocytosis and recycling of cholecystokinin receptor type A, *J Biol Chem*, **272**:14817-14824.

Vazquez-Prado, J., Medina, L. C., Romero-Avila, M. T., Gonzalez-Esponiso, C., and Garcia-Sainz, J. A. (2000) Norepinephrine- and phorbol ester-induced phosphorylation of $\alpha_{1a}$-adrenergic receptors, functional aspects, *J. Biol. Chem,* **275**:6553-6559

Molecular Pharmacology Fast Forward. Published on December 30, 2004 as DOI: 10.1124/mol.104.008417
This article has not been copyedited and formatted. The final version may differ from this version.



**Figure legends**

**Figure 1. Affinities of compounds measured by [$^3$H]-prazosin competition binding in R-1Fs stably expressing $\alpha_{1a}$-AR**

Competition between [$^3$H]-prazosin, (0.2 nM) and increasing concentrations of phenylephrine, (circles, n=4), QAPB, (open circles, n=6) and prazosin (squares, n=4) for binding to membranes prepared from R-1Fs expressing the bovine $\alpha_{1a}$-AR. Assay points were determined in triplicate and non-specific binding was determined in the presence of phentolamine (10 μM). The $pK_i$ and nH values for these compounds are listed in Table 1.

**Figure 2. Direct visualization of the fluorescent ligand-$\alpha_{1a}$-AR complex and co-localization of the fluorescent ligand with human $\alpha_{1a}$-AR-EGFP2 in HEK293T cells**

(A) Hoechst (blue) stained nuclei and the level of QAPB (10 nM) fluorescence detected from the same field in non transfected HEK293T cells is shown in image i and ii respectively. (B) Human $\alpha_{1a}$-AR was expressed transiently in HEK293T cells and its distribution visualized after 75 min exposure to 10 nM QAPB (green colour in overlay image of panel B). (C) Human $\alpha_{1a}$-AR-EGFP2 was expressed transiently in HEK293T cells. Image i shows the distribution of EGFP2 and image ii shows the localization of RQAPB (10 nM) after 75 min exposure to the fluorescent antagonist ligand. Co-localization of the EGFP2 fusion protein and RQAPB is represented by yellow/orange colour in overlay image iii of panel C. (D) 3D overlay maximum projection view of intracellular fluorescent $\alpha_{1a}$-AR/QAPB ligand sites (green punctate vesicles) and Hoechst stained nuclei (blue colour) in R-1Fs is shown in images i-iii: (i) x-y view, (ii) x-z view and (iii) y-z view.

**Figure 3. Separation of $\alpha_{1a}$-ARs in intracellular pools and at the cell surface and comparison of the changes in the distribution of fluorescent QAPB intensity during equilibration binding of QAPB and during loss of QAPB from recycling $\alpha_{1a}$-ARs stably expressed in R-1F cells**

(A) Time-lapse images presented show the development of QAPB, (5 nM), fluorescence to steady-state. Asterisk superimposed on image i of Fig. 3A represents the link to supplemental QuickTime movie 1, (prepared from assembled time lapse images of image i over 75 min ), which can be viewed at

http://molpharm.aspetjournals.org. Movie 1 revealed that some of the QAPB labelled receptors displayed short range bi-directional motion, whereas others were inert, or moved vast distances.

Image i represents the cell autofluorescence at 0 time, (i.e. prior to the addition of QAPB. Image ii shows surface QAPB fluorescence, (at 2 min). Image iii represents the distribution of surface and intracellular receptor QAPB fluorescence after 4 min exposure to the QAPB ligand. The distribution of surface and intracellular QAPB fluorescence at steady-state is shown in image v.

(B) Time lapse images presented in panel B show a more sharpened view of the mobile intracellular organelles images when surface QAPB fluorescence binding at 2 min, (Fig. 3A, image ii), is subtracted from the time series images presented in panel A.

(C) Fluorescent intensity histogram of QAPB fluorescence distribution over time (bins 2-9 shown). Histogram shows the distribution pattern continually changes as QAPB equilibrates with recycling $\alpha_{1a}$-ARs. Bin 1 (not shown) contains all the black pixels and background noise except a very small number that appear in Bin 2; at time zero no other Bin contains any pixels. Equilibration of QAPB with cycling $\alpha_{1a}$-ARs was detected as a progressive shift to the right, indicating the gradual appearance of steadily brighter pixels until equilibrium is reached.

(D) Loss of QAPB fluorescence over a 80 min wash period is shown in image i-vi.

**Figure 4. Time course of the distribution of fluorescent QAPB intensity measured at steady-state and during loss of QAPB from cycling $\alpha_{1a}$-ARs in R-1Fs**

(A) Fluorescent intensity time course plot of onset of QAPB fluorescence binding over time, (bins 2-8 shown, data reanalysed from Fig 3C). (B) Washout: the time course plot during loss of QAPB from recycling receptors (bins 2-8 shown). (C) The development of total fluorescence, (over time), associated with the binding of the QAPB ligand to $\alpha_{1a}$-ARs to a steady-state within 55 min. Black solid line corresponds to the total (surface and intracellular) QAPB fluorescence whereas the broken black line represents the intracellular component after subtracting the surface binding represented by the fluorescence at 2 min (see image subtraction protocol outlined in methods).

Molecular Pharmacology Fast Forward. Published on December 30, 2004 as DOI: 10.1124/mol.104.008417
This article has not been copyedited and formatted. The final version may differ from this version.



**Figure 5. Recycling $\alpha_{1a}$-AR-QAPB ligand complexes are displaced by the competitive $\alpha_1$-antagonist ligand phentolamine in R-1Fs stably expressing $\alpha_{1a}$-AR**

(A) Images i and ii show equilibrium binding of QAPB (5 nM) to recycling bovine $\alpha_{1a}$-AR over 15 min, (cell exposed to QAPB for 90 min in total). The images are non-identical because the endosomes are mobile but total fluorescence is constant. (iii) phentolamine (10 μM, 240 min) almost abolishes fluorescence, (iv) phentolamine 100 μM (a further 120 min) abolishes fluorescence. (B) Time course of loss of QAPB (5 nM) for 75 min) fluorescence caused by wash, phentolamine or both; pooled data, mean ± S.E.M. Black trace illustrates the rate of loss on washing with QAPB-free saline (n=3). Dark grey line shows a faster rate of loss in QAPB-free saline with phentolamine (100 μM, n=3). Phentolamine (100 μM) given in the continued presence of QAPB (5 nM) produced complete displacement but took longer than when QAPB was removed (light grey trace, n=4).

**Figure 6. Blockade of QAPB fluorescence binding to recycling $\alpha_{1a}$-ARs by concanavalin A and hyperosmotic sucrose, but not filipin in R-1Fs**

R-1Fs stably expressing $\alpha_{1a}$-ARs were pre-equilibrated with QAPB (5 nM) for 90 min at room temperature. Graph presented is pooled normalized data showing that pre-incubation of the R-1Fs with Con A (0.25 mg/ml); (black bar, (n=5) or hyperosmotic sucrose (0.45 M); (grey bar, n=5), but not filipin (5 μg/ml); (dotted black bar, n=3, shown only at 90 min), significantly ($p<0.001$) inhibits QAPB binding to $\alpha_{1a}$-ARs. *$p<0.001$, Con A or sucrose data (30, 60 & 90 min) versus normalized QAPB fluorescence data (measured upon initial equilibrium binding of QAPB, value set to 1). †, $p<0.001$, filipin versus Con A or sucrose data.

**Figure 7. Internalization of $\alpha_{1a}$-AR-EGFP2 in MEF cells is β-arrestin-dependent**

(A) β-arrestin 1/2 deficient MEF cells were transiently transfected with an $\alpha_{1a}$-AR-EGFP2 fusion protein. Images i and ii show that the $\alpha_{1a}$-AR-EGFP2 fusion protein was predominantly expressed inside the cell in a clustered vesicular arrangement (green colour, white arrows) with a lower level of expression localized on the membrane surface (light green colour, red arrows). Nuclei are shown in blue. Asterisk on image i of Fig. 7A represents the link to movie 2 prepared from assembled time lapse

Molecular Pharmacology Fast Forward. Published on December 30, 2004 as DOI: 10.1124/mol.104.008417
This article has not been copyedited and formatted. The final version may differ from this version.



images of image i recorded at 15 sec intervals. Movie 2 indicated that the intracellular, clumped pool of $\alpha_{1a}$-AR-EGFP2 was motionless, in contrast with observations in wild type MEF cells.

(B) Blue, green and red colours in images i to iii show the location of cell nuclei, $\alpha_{1a}$-AR-EGFP2 fusion protein and RQAPB (10 nM), respectively in β-arrestin 1/2 deficient MEFs after pre-incubation with RQAPB for 75 min. Overlay image iv shows that although RQAPB (10 nM) can bind to cell surface $\alpha_{1a}$-AR-EGFP2 (red arrow, yellow represents co-localization), it cannot access the intracellular pool (green colour, white arrows). Asterisk on top of overlay image iv of Fig. 7B represents the link to movie 3 showing a 3D y-z animated view of this image. Movie 3 clearly shows the RQAPB ligand-$\alpha_{1a}$-AR–EGFP2 complex (yellow) only on the surface of the MEF cell.

(C) Wild type, β-arrestin 1/2 expressing, MEFs. Images i to iii are analogous to those in panel B. The cells show a more "normal" distribution of GFP-labelled receptors, i.e. with membrane and intracellular punctuate distribution as in HEK 293 and R-1F cells. Asterisk on overlay image iv of panel C of Fig. 7 represents the link to movie 4 showing a 3D animated y-z view of this image. Movie 4 shows clearly that the RQAPB ligand internalized and co-localized with surface (red arrow) and intracellular (white arrow) $\alpha_{1a}$-AR-EGFP2 (Fig. 7C, image iv). Non transfected wild type MEFs (e.g. nucleus at bottom left of panel with no associated GFP) display no RQAPB fluorescence, serving as another control.

**Figure 8. Localization of β-arrestin 2-EGFP is agonist-independent and it partially colocalizes with RQAPB-labelled $\alpha_{1a}$-ARs**

R-1Fs stably expressing bovine $\alpha_{1a}$-ARs were transiently transfected with β-arrestin 2-EGFP. 24 h after transfection multi-fluorescence images were acquired from the same field of view. (A) [i] Green vesicles represent the non-uniform, cytoplasmic localization of β-arrestin 2-EGFP with intense β-arrestin 2-related fluorescence expressed in punctate vesicles, (some shown by white arrows). Asterisk overlayed on image i of Fig 8A represents the link to movie 5 prepared from reconstructed sequential time lapse 2D-images of image i recorded at 15 sec intervals. Movie 5 demonstrated that the organelles containing β-arrestin 2-EGFP showed rapid movement around the cells similar to that found for organelles carrying $\alpha_{1a}$-ARs. Images ii to iii show that after 15 min exposure to the agonist phenylephrine, (PE), (3 μM), no change in the localization of β-arrestin 2-EGFP2 was observed. (B)

Molecular Pharmacology Fast Forward. Published on December 30, 2004 as DOI: 10.1124/mol.104.008417
This article has not been copyedited and formatted. The final version may differ from this version.



Co-localization of RQAPB-labelled bovine $\alpha_{1a}$-ARs with β-arrestin 2-EGFP. [i] Blue colour represents cell nuclei. [ii] Green colour shows the localization of β-arrestin 2-EGFP2. Image iii depicts the RQAPB pattern of fluorescence. [iv] Overlay image shows partial constitutive association (yellow/orange vesicles, some shown by white arrows) of bovine $\alpha_{1a}$-AR-RQAPB ligand complexes with β-arrestin 2-EGFP. In the red rectangular region superimposed on images ii-iv a pixel-by-pixel correlation of EGFP and RQAPB fluorescence was made (see text).

**Figure 9. Internalized QAPB ligand-$\alpha_{1a}$-AR-complexes co-localize with recycling and late endosomal fluorescent markers in R-1Fs stably expressing $\alpha_{1a}$-AR**

(A) Co-localization with recycling compartments. [i] Green punctates represent QAPB (10 nM) labelled $\alpha_{1a}$-ARs and blue colour shows nuclei stained with Hoechst. [ii] Recycling vesicles labelled with Tfn-Alexafluor$^{546}$ are represented by the red punctate spots. [iii] Overlay image showing partial co-localization, (yellow perinuclear vesicles) of bovine $\alpha_{1a}$-AR-QAPB ligand complexes with the recycling endosomal marker. [iv] 3D x-z overlay maximum projection view, where yellow vesicles, (some shown by white arrows), represent co-localization of QAPB-labelled bovine $\alpha_{1a}$-ARs with the recycling marker. (B) Co-localization with late endosomes. [i] Green punctates represent QAPB (10 nM) labelled $\alpha_{1a}$-ARs. [ii] Late endosomes labelled with Lysotracker Red are represented by the red punctate vesicles. [iii] Red and green overlay image where yellow punctates represent co-localization of QAPB labelled bovine $\alpha_{1a}$-AR with the late endosomal marker. [iv] 3D x-z overlay maximum projection view of bovine $\alpha_{1a}$ -AR-QAPB ligand complexes co-localizing with the late endosomal marker (yellow vesicular structures, some represented by white arrows).

Molecular Pharmacology Fast Forward. Published on December 30, 2004 as DOI: 10.1124/mol.104.008417
This article has not been copyedited and formatted. The final version may differ from this version.



**Tables**

**Table 1. Radioligand binding affinity and Hill slope estimates**

| Ligand | $pK_i$ | nH | N |
|---|---|---|---|
| **Prazosin** | **9.26 ± 1.33** | **0.91 ± 0.15** | **4** |
| **QAPB** | **9.14 ± 1.70** | **1.08 ± 0.11** | **6** |
| **Phenylephrine** | **5.70 ± 0.32** | **0.78 ± 0.10** | **4** |

$pK_i$ values (means ± S.E.M.) and nH were evaluated for each test ligand. Values of N represent the number of individual experiments.

Molecular Pharmacology Fast Forward. Published on December 30, 2004 as DOI: 10.1124/mol.104.008417
This article has not been copyedited and formatted. The final version may differ from this version.



**Table 2. Association and dissociation rate constant estimates of the development and loss of QAPB fluorescence from cycling $\alpha_{1a}$-ARs**

| Ligand | Total ($min^{-1}$) | Total t½ min | Intracellular ($min^{-1}$) | Intracellular t½ min |
|---|---|---|---|---|
| **Control** | | | | |
| **Association** | **0.0802± 3.865e-004** | **12.47** | **0.0807 ± 3.587e-004** | **12.39** |
| **Dissociation** | **0.0824 ± 3.137e-004** | **12.14** | **0.1040 ± 1.9207e-004** | **9.61** |
| **Wash (-PTA)** | | | | |
| **Dissociation** | **0.046 ± 2.51e-004** | **22.00** | | |
| **Wash (+PTA)** | | | | |
| **Dissociation** | **0.094 ± 3.41e-004** | **10.70** | | |
| **Wash (+QAPB, +PTA)** | | | | |
| **Dissociation** | **0.039 ± 2.04e-004** | **25.60** | | |

K values are represented as the mean ± S.E.M , PTA = phentolamine

Molecular Pharmacology Fast Forward. Published on December 30, 2004 as DOI: 10.1124/mol.104.008417
This article has not been copyedited and formatted. The final version may differ from this version.

**Fig. 1**

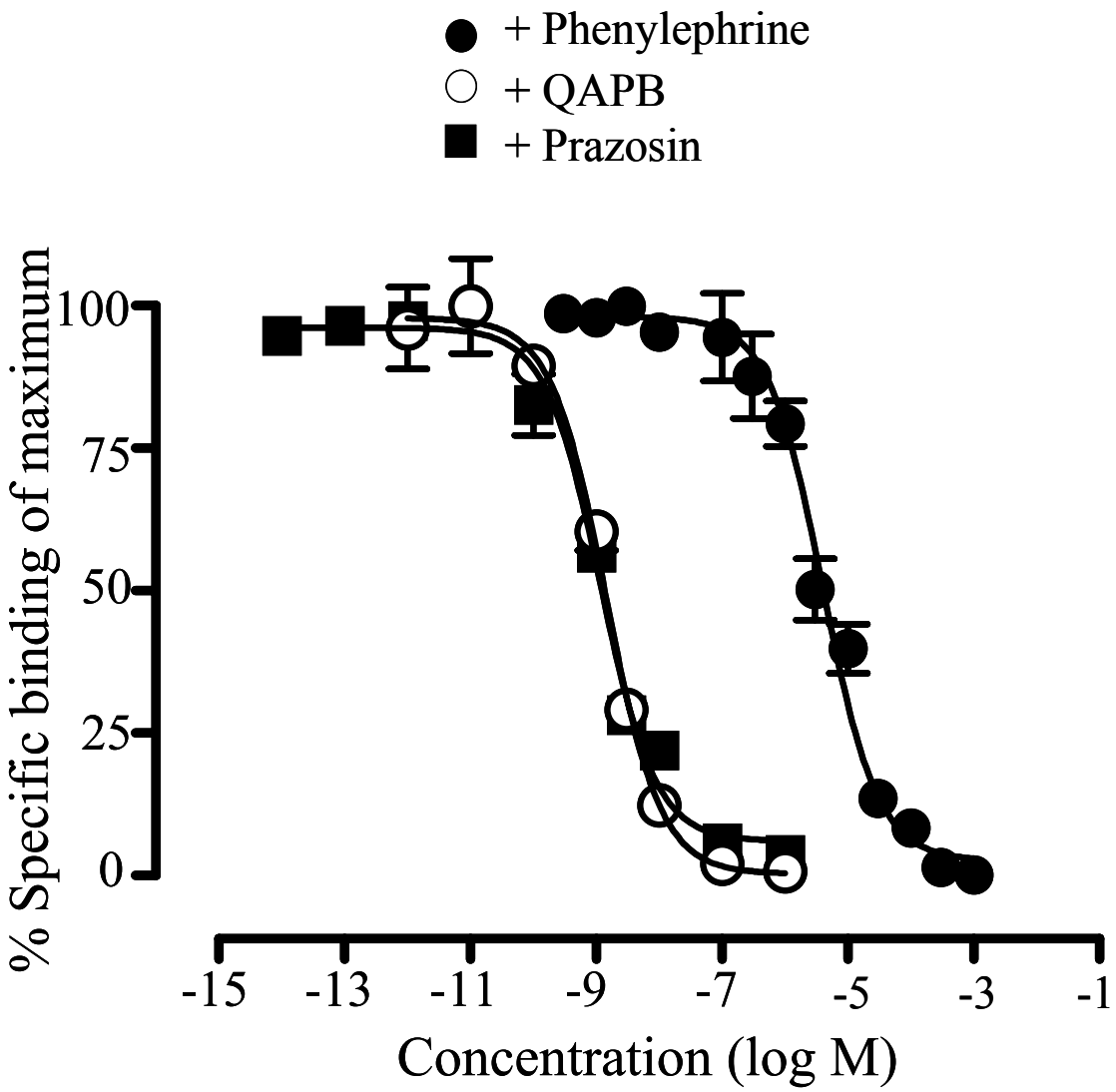

Molecular Pharmacology Fast Forward. Published on December 30, 2004 as DOI: 10.1124/mol.104.008417
This article has not been copyedited and formatted. The final version may differ from this version.

**Fig. 2**

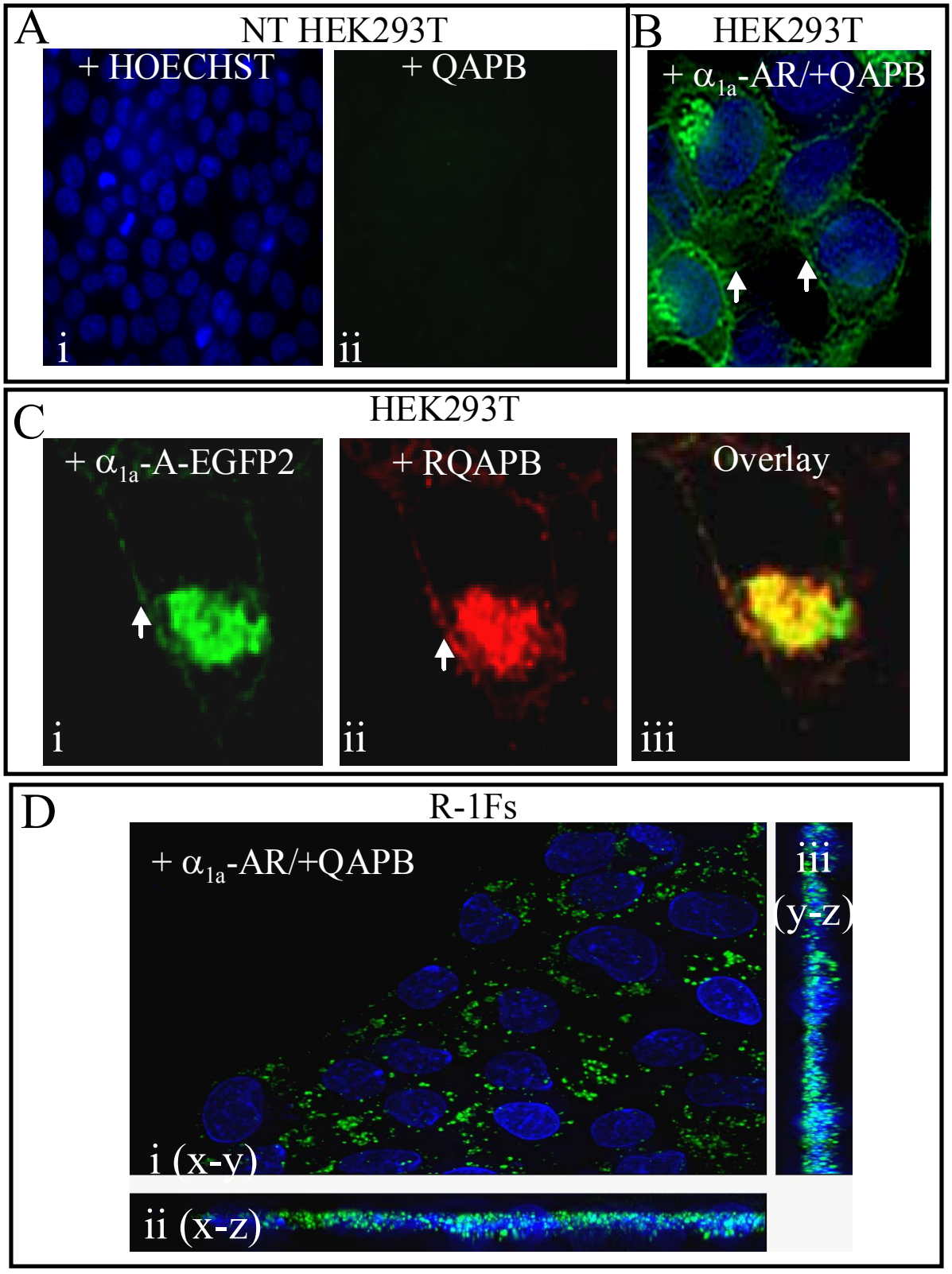

Molecular Pharmacology Fast Forward. Published on December 30, 2004 as DOI: 10.1124/mol.104.008417
This article has not been copyedited and formatted. The final version may differ from this version.

**Fig. 3**

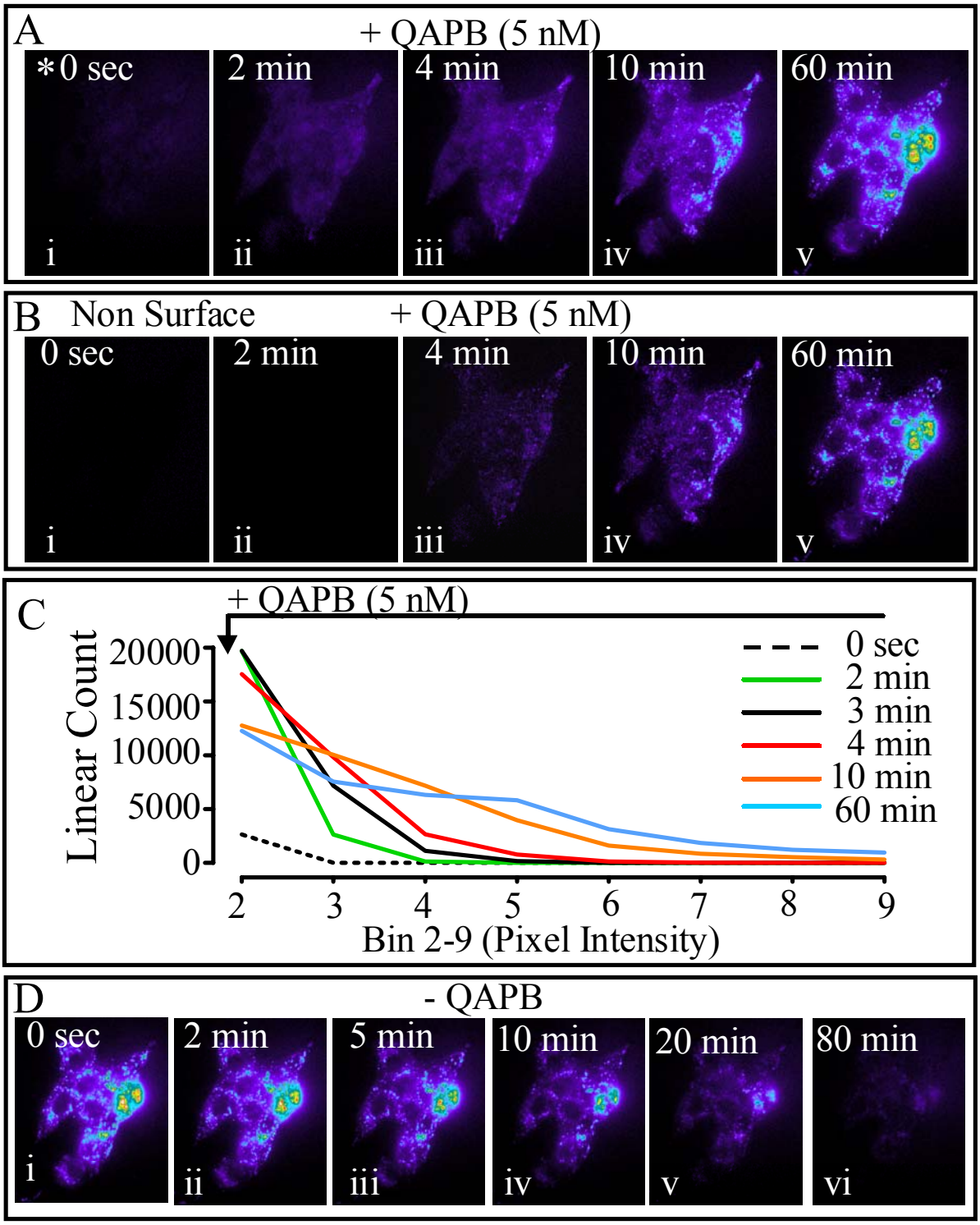

Molecular Pharmacology Fast Forward. Published on December 30, 2004 as DOI: 10.1124/mol.104.008417
This article has not been copyedited and formatted. The final version may differ from this version.

**Fig. 4**

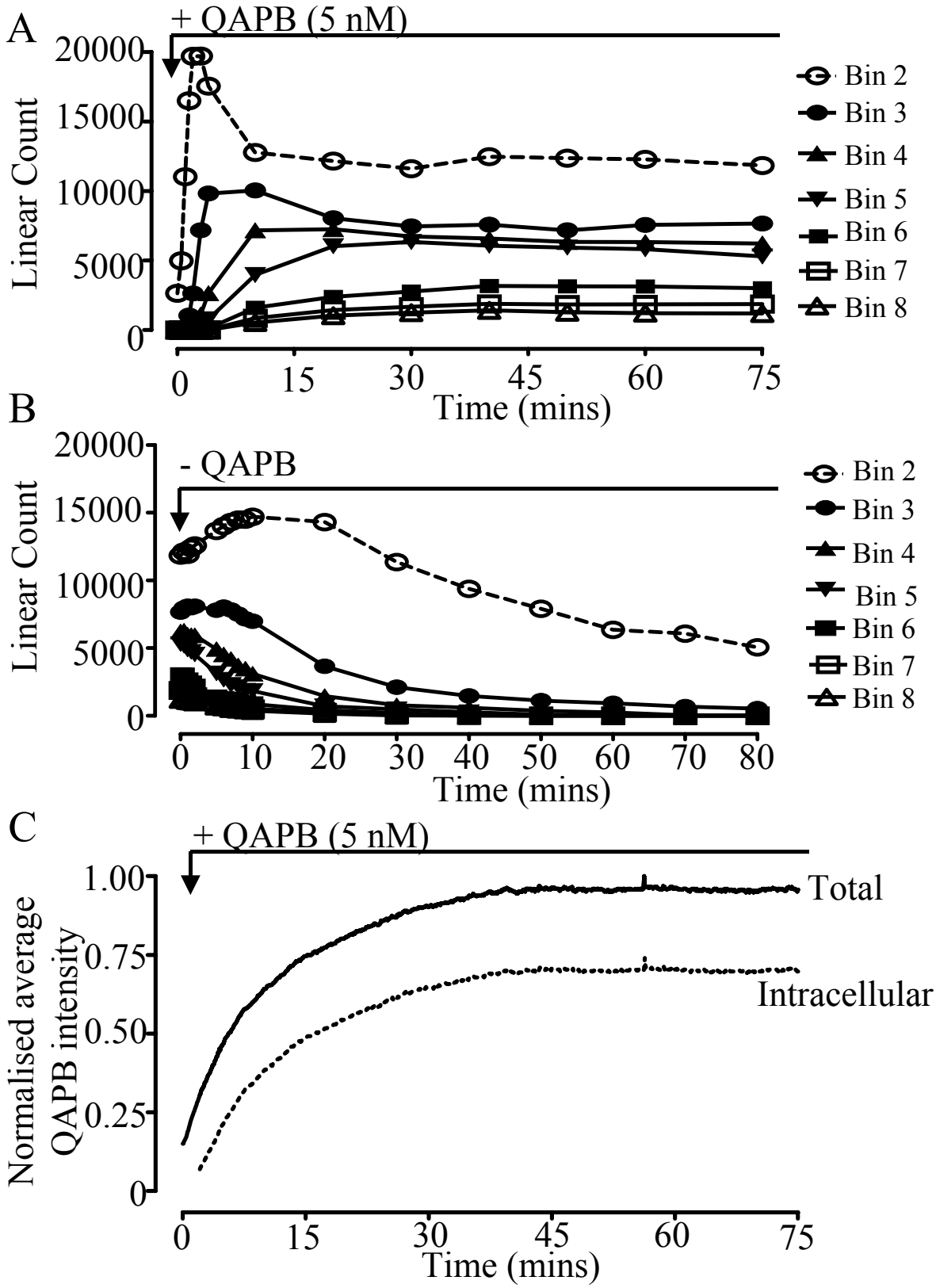

Molecular Pharmacology Fast Forward. Published on December 30, 2004 as DOI: 10.1124/mol.104.008417
This article has not been copyedited and formatted. The final version may differ from this version.

**Fig. 5**

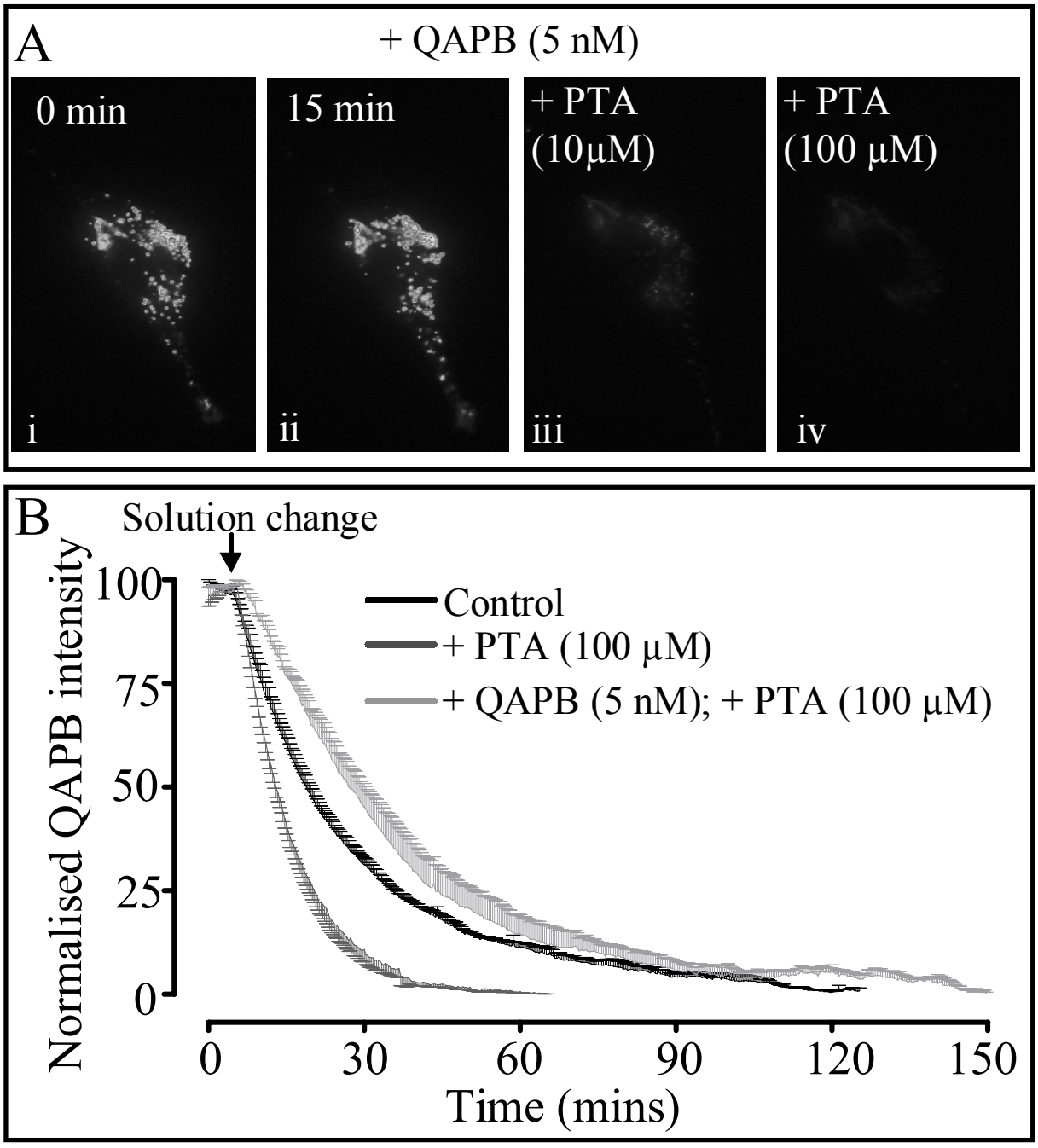

Molecular Pharmacology Fast Forward. Published on December 30, 2004 as DOI: 10.1124/mol.104.008417
This article has not been copyedited and formatted. The final version may differ from this version.

**Fig. 6**

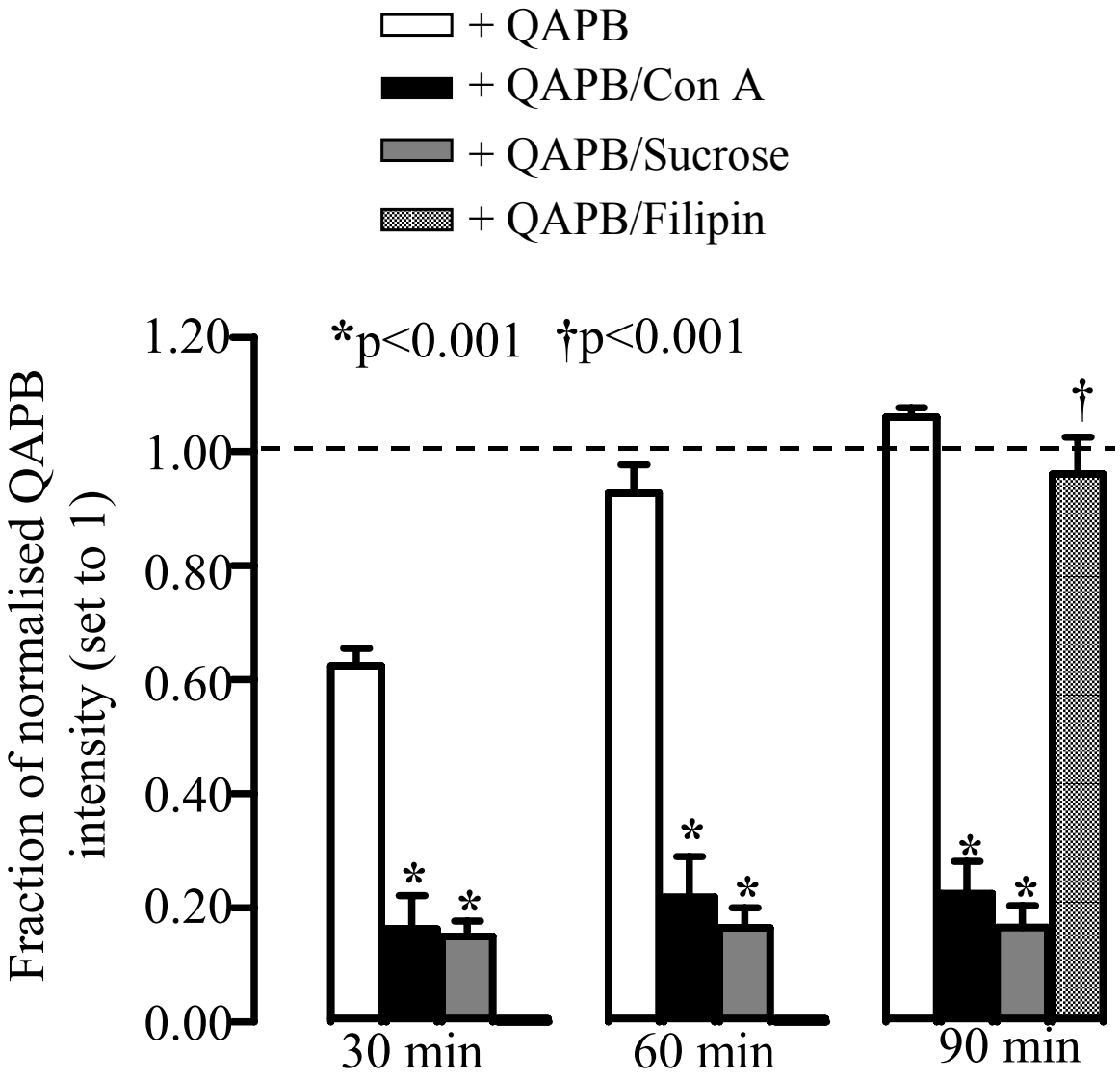

Molecular Pharmacology Fast Forward. Published on December 30, 2004 as DOI: 10.1124/mol.104.008417
This article has not been copyedited and formatted. The final version may differ from this version.

**Fig. 7**

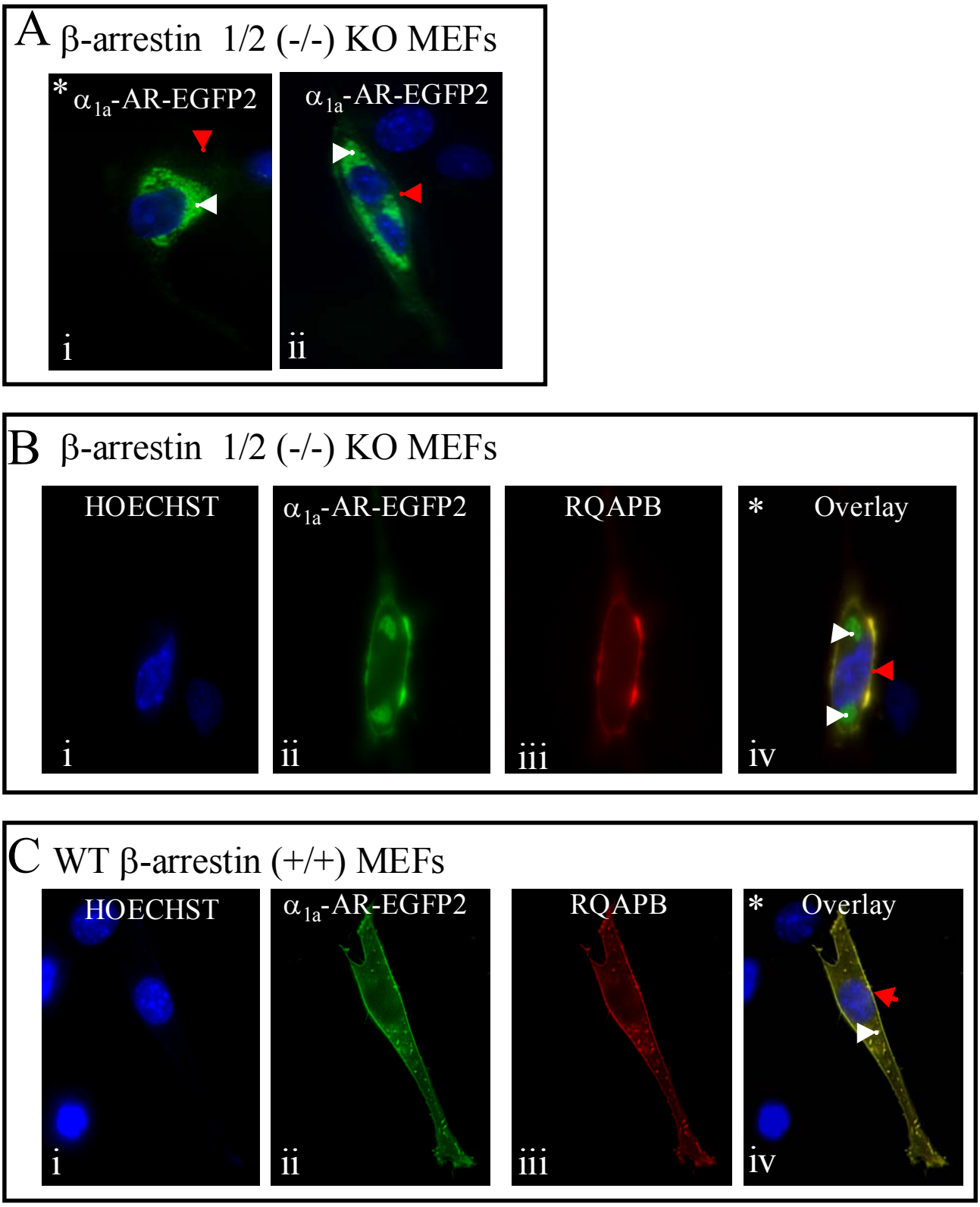

Molecular Pharmacology Fast Forward. Published on December 30, 2004 as DOI: 10.1124/mol.104.008417
This article has not been copyedited and formatted. The final version may differ from this version.

**Fig. 8**

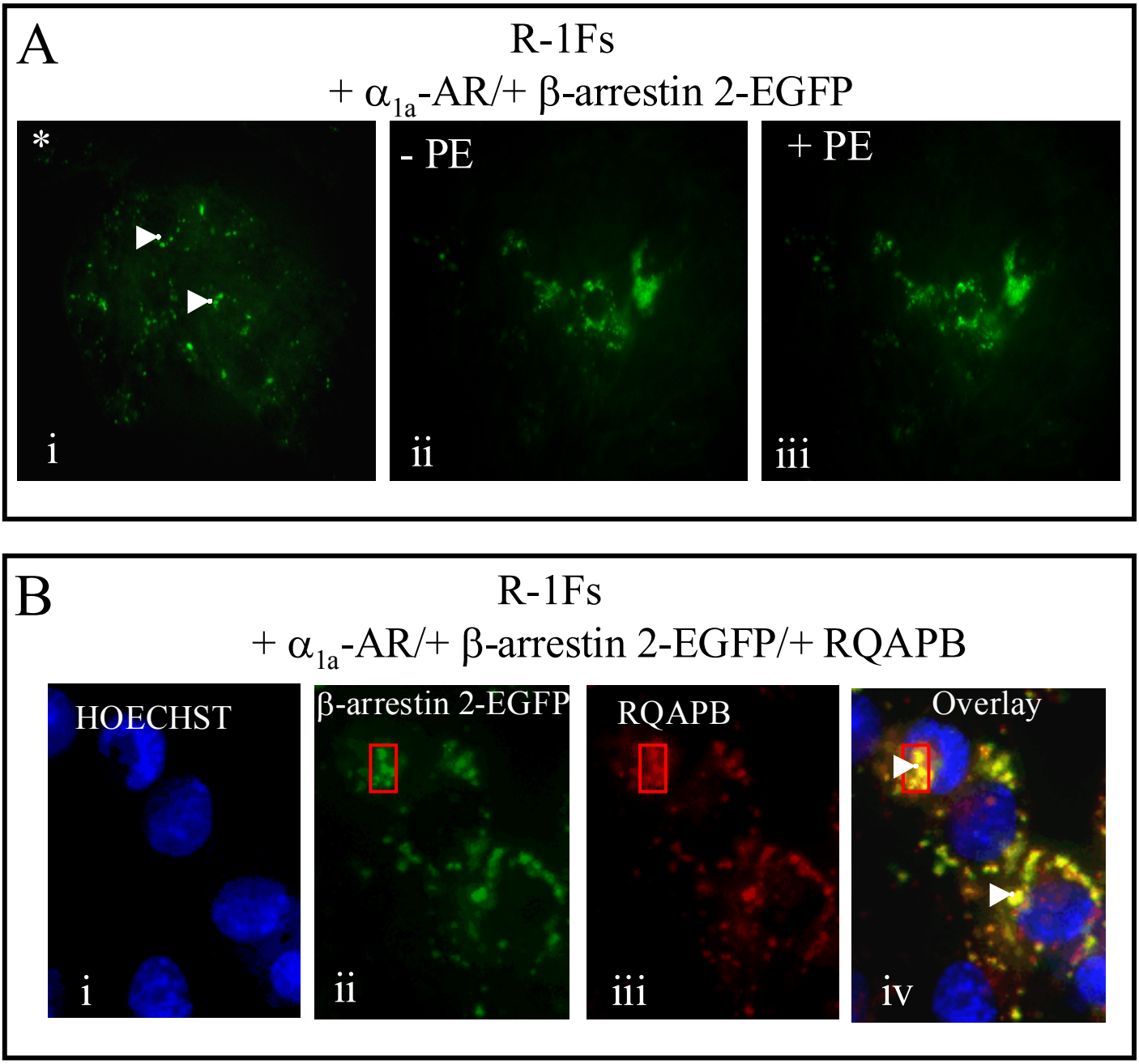

Molecular Pharmacology Fast Forward. Published on December 30, 2004 as DOI: 10.1124/mol.104.008417
This article has not been copyedited and formatted. The final version may differ from this version.

**Fig. 9**